



**HAL**  
open science

## **Experimental analysis of mechanical performance of glass fibre reinforced polyamide 6 under varying environmental conditions**

Ivanna Pivdiablyk, Patrick Rozycki, Frédéric Jacquemin, Laurent Gornet, Stéphane Auger

### **► To cite this version:**

Ivanna Pivdiablyk, Patrick Rozycki, Frédéric Jacquemin, Laurent Gornet, Stéphane Auger. Experimental analysis of mechanical performance of glass fibre reinforced polyamide 6 under varying environmental conditions. *Composite Structures*, 2020, 245, pp.112338. <10.1016/j.compstruct.2020.112338>. <hal-05250553>

**HAL Id: hal-05250553**

**<https://hal.science/hal-05250553v1>**

Submitted on 18 Sep 2025

**HAL** is a multi-disciplinary open access archive for the deposit and dissemination of scientific research documents, whether they are published or not. The documents may come from teaching and research institutions in France or abroad, or from public or private research centers.

L'archive ouverte pluridisciplinaire **HAL**, est destinée au dépôt et à la diffusion de documents scientifiques de niveau recherche, publiés ou non, émanant des établissements d'enseignement et de recherche français ou étrangers, des laboratoires publics ou privés.



Distributed under a Creative Commons CC BY-NC 4.0 - Attribution - Non-commercial use - International License

## Experimental analysis of the mechanical performance of glass fibre reinforced 6 under varying environmental conditions.

Ivanna Pivdiablyk\*<sup>1</sup>, Patrick Rozycki<sup>1</sup>, Frédéric Jacquemin<sup>2</sup>, Laurent Gornet<sup>1</sup>, Stéphane Auger<sup>3</sup>

<sup>1</sup>Research Institute in Civil and Mechanical Engineering (GeM), Ecole Centrale de Nantes, 1 Rue de la Noë, 44300 Nantes, France

<sup>2</sup>Research Institute in Civil and Mechanical Engineering (GeM), Université de Nantes, 58 Rue Michel Ange, 44600 Saint-Nazaire, France

<sup>3</sup>Technical Centre for Mechanical Industry (CETIM), 74 Route de la Jonelière, 44000 Nantes, France

### Abstract

The polyamide-based composite materials are widely employed in various industrial domains. Along with the numerous advantages of these engineering materials, an important sensitivity to hygrothermal conditions represents a major drawback. Hence, this study **aims** to thoroughly evaluate the variation of physical and mechanical properties in moist and thermal environments of three stacking sequences. An extensive tensile testing campaign is performed in order to create a rich experimental database. It is therefore preceded by a proper establishment of desiccation/absorption protocol for the composite material. The results demonstrate that the humid ageing parameters are highly affected by the temperature. The mechanical response is dependent on the glass transition temperature, or  $T_g - T$  criterion, due to the occurring material plasticisation as a result of absorbed moisture. The shear modulus, the shear yield stress and strength deteriorate with the increase of temperature and moisture content. The changes of properties for the longitudinal and transversal orientations are not considerably pronounced.

### Keywords

\* Corresponding author. Address: Ecole Centrale de Nantes, 1 Rue de la Noë, 44300 Nantes, France. Tel.: +330240372579.

*E-mail address:* ivanna.pivdiablyk@ec-nantes.fr (I. Pivdiablyk)

A. Polymer-matrix composites (PMCs); B. Hygrothermal effect; Mechanical properties; C. Elastic properties; Tensile testing

## **1 Introduction**

### **1.1 Research interests**

Mechanical, bonding and thermal connections are widely employed in the automobile, aeronautical, marine and energy industries. Bolted joints occupy a significant segment among other mechanical assemblies, particularly through the possible preload application. Conception and computation of such connections are widely performed according to a European standard NF E 25030-2. The standard-based software CETIM-Cobra is therefore used by numerous enterprises with the limitation to metallic materials in terms of a homogeneous structure and elastic properties. An intensive application of the composite materials with superior mechanical and physical properties leads to an expansion of the previous standard towards the heterogeneous materials [1]. However, the effect of environmental conditions (moist and temperature) should also be accounted for due to the high sensitivity of some composites. Thus, the present article deals with **one** part of our research based on the determination of both temperature and humidity impacts on a Glass/PA6 woven composite material; **the other** part, related to the Representative Volume Element (RVE) modelling for numerical simulations of out-of-plane parameters, **will be the subject of a second paper. The complete study is**, firstly, required to complete the evaluation of mechanical properties, and, secondly, to define the mechanical behaviour of bolted joints over time. Eventually, these analyses and results will be integrated into the software CETIM-Cobra in order to manage the sensitivity of the composite material to given environmental conditions.

### **1.2 Environmental conditions**

Components of vehicles are required to sustain a wide range of temperatures, from  $-40^{\circ}\text{C}$  to  $+80^{\circ}\text{C}$ , and dry or humid environments in order to fulfil their functions. These conditions are of high concern for polyamide 6 as an engineering material itself and also as a constituent in composite materials. Polyamide-based composite materials are employed in numerous parts for the subsequent implementations in the automobile industry, for instance, clutch pedals, clutch master cylinders, steering wheel, levers, seat frames, cooling fans, rocker box covers, air filter nozzle etc., so they endure an important hydrothermal mechanical impact [2,3].

Prolonged exposure to harsh environments provokes physical and mechanical deterioration severely [4,5]. Fibres, except organic, are presumed not to undergo important changes at high/cold temperatures and humid climate [6,7], whereas a resin degradation can be crucial up to the loss of its primary functions – fibre bonding and protecting. Consequently, a loss of expected properties is likely to occur with the Glass Fibre reinforced PA6 composite as well.

Polyamide 6 intensively absorbs water due to the presence of amide groups  $-\text{HN}-$  in the amorphous part of the polymer. At first, water molecules occupy the free space, i.e. the free volume, and then interact with hydrogen bonds. A certain quantity of accumulated molecules or clusters induces the activation of chain mobility and decreases the attraction between molecules, leading to the flexibility of the polymer. This chemical interaction explains the material sensitivity resulting in plasticisation and physical degradation [8].

Starkweather [9] is one of the pioneers who commenced examining nylons in moist environments. He discovered the quasi-linear relation between dimensional expansion and mass changes of polyamide 66 due to humidity. It is, however, valid on a large scale, and, as demonstrated by Wei et al. [10], some non-linearities are present at the beginning of the water sorption. Such behaviour can be explained by an initial occupation of a present free volume that does not contribute to noticeable expansion. It is worth mentioning that the water molecules are not homogeneously distributed throughout a material thickness and length,

hence, creating water profiles. Nevertheless, the longitudinal and out-of-plane deformations are coherent to the present water content [11–14]. Such time-dependent water profile is affected by a diffusion coefficient and boundary conditions, whereas the time to desiccation/saturation is also determined by material geometry and properties. The complexity of specimen geometry on the water uptake is investigated and demonstrated in [15–17]. They assign it to the non-linear relation of the specimen thickness and time to saturation. Also, the authors clearly show that an addition of a few composite layers leads to a significant increase in time, needed to obtain a required material condition.

The effect of **Relative Humidity** (RH) on the absorbed amount of moisture by PA6 and its kinetics was studied by [15,18]. The authors show that the linearity only exists until an approximate threshold of 85% of RH. Beyond this value, the slope increases, illustrating a more important uptake capacity. Silva et al., Starkova et al. [19,20] explored the effect of temperatures from +20°C to +90°C on the absorption and desorption kinetics by proving that the saturation and the complete desiccation occur the fastest at +90°C. Yet, the amounts of absorbed and then consequently released water at the same temperature are not equal. Hence, the authors relate this phenomenon to the bound water of the Langmuir model. Results in [21] are in accordance in terms of the moisture absorption kinetics.

The glass transition temperature is the subject of numerous articles. This temperature provokes a polymer transformation from solid and glassy, if below, to viscous and rubbery state if above. Besides,  $T_g$  of polyamides is highly dependent on the content of absorbed water. For instance, Kaimin et al. [22] analysed its dependence on the moisture content of an oriented polycapromamide. A drop in  $T_g$  is nearly +70°C: from +60°C for a dry material to around -10°C when containing approximately 9% of moisture. Similar results were likewise obtained in [11,23–25] for the other polyamides.

Relevant studies towards the understanding of the water-induced mechanical changes of neat and reinforced PA6 were carried out in [15,19,21,23–27]. The growing water uptake significantly affects the yield stress and Young's modulus that tend to a remarkable decrease of around 80-90% when the water content is about 9%. Hence, the linear elastic region is clearly visible up to 1.7% of water content, but above this limit, the plastic region is greatly pronounced. The analysis of the in-plane tensile extension, demonstrated in [15,21,26,27], shows the non-linear relation between the tensile strain at rupture and the moisture content or RH. The tensile strain is assumed to increase with water content till an admissible level of the latter, after which the strain tends to reduce. Besides, not only the presence of water molecules entails the degradation of mechanical properties, but also the temperature as stated by Lyons [28], which is attributed to increased chain mobility. Hence, the overall drop in mechanical properties can be linked to altering  $T_g$  due to moisture and temperature impact as proposed by Reimschuessel [25].

Modifications of the material properties, mentioned above, are physical and remain reversible [29,30]. Nevertheless, chemical damage, of non-reversible nature, can also take place. For instance, hydrolysis can be caused by prolonged immersion into water or exposure to humid air at elevated temperatures. It results in a chain scission of the polymer followed by the irreversible reduction of mechanical characteristics. Bernstein et al. [31] investigated the effect of time of thermo-oxidative ageing and hydrolytic ageing in oxygen on the tensile strength of PA66. Indeed, the mechanical performance of the resin is strongly reduced at high and low temperatures, moisture and the duration of exposure. The comparable conclusion is made in [23] for the neat PA6 resin. They determined the molar weights of specimens with the following conditions: unaged, aged in seawater for six months and also dried after ageing. No significant changes were found. For these reasons, the chemical damage is not considered

in the current work by cause of shorter exposure time at lower temperatures than studied by the above-mentioned authors.

Despite a **great** number of published papers on the environmental impact on composite materials with thermoplastic or thermoset **matrices**, the lack of information regarding a consistent **conditioning** and testing **procedures** represents an **essential** drawback for industrial and scientific fields. Above-mentioned analysis of mechanical and physical properties of a neat and glass-fibre reinforced PA6 in hygrothermal conditions leads to **the** necessity of a more profound characterisation. Also, a clear understanding of changing characteristics can lead to a better design of composite elements, **in particular in the context of composite bolted structures**. Hence, this study deals with the environmental effect on the durability of the composite PA6 GF.

The present paper is composed of two distinct sections that are based on experimental analysis. The first part is related to the development of a conditioning protocol, i.e. desiccation and humid ageing of the given composite material. This long-term study allows authors to ensure the necessary moisture content in the specimens. In addition, the suggested duration of desorption and absorption is relatively short; thus, they could be adopted for industrial purposes. To complete the material state identification, the glass transition temperature is evaluated for three moisture contents. The tensile testing campaign represents **the second part of the article**. The tensile material properties are reported for three fibre orientations using both “true” stress and strain characteristics due to large strains. Negative and positive temperatures as well as three moisture contents, affecting the durability, are accounted for the testing campaign to evaluate the properties at yield and rupture. **The selected conditions are standard for automotive applications and allow the creation of a relevant database.**

## **2 Material description and specimen preparation**

The study is based on a composite PA6 GF – polyamide 6 reinforced with continuous roving glass fibres of a trademark Tepex® Dynalite, supplied by LANXESS group. The reinforcement is used in the form of fabric with a twill weave 2×2 and equal weight rate in both longitudinal and transverse orientations. Laminate is delivered in the form of plates of a total thickness of 2 mm. The thickness of each layer is 0.5 mm. The fibre volume content is 47%. The laminate was then stored under unregulated environmental conditions for nearly three years. Consequently, its state, for instance, the moisture content and mechanical behaviour, is unknown.

Specimens, used in the present work, are of two geometries. They were cut out from two sheets, produced within one manufacturing process, with a water jet according to demanded dimensions and fibre orientation. All the specimens were then referenced and stored in ambient environmental conditions until the testing campaign. After the desiccation/absorption procedures, the specimens were placed into aluminium vacuum storage bags according to the testing batches (section 4).

### 2.1 45° fibre orientation

The first type of specimens is of rectangular geometry 250 mm × 25 mm × 2 mm (Figure 1). The fibre orientation is 45°. In terms of application, they are used for the characterisation of moisture content and the determination of in-plane shear properties in the tensile testing campaign. No recommendation is given for the specimen geometry of woven composites. However, it remains mandatory to consider the size of RVE, thus at least 1.5 of an RVE should be in the effective width. Therefore, the chosen specimen contains nearly 2.4 of RVE oriented at 45°.

Considering the further temperature and moisture treatment, the glue under the end-tabs may appear sensitive. It can, thus, lead to the sliding between a specimen and the end-tabs

during traction. In order to prevent the side effects, it is decided to renounce the end-tabs despite the suggestion of ISO 527-5.

## 2.2 0° and 90° fibre orientations

The specimens of 0° and 90° fibre orientations of the standard geometry (Figure 1) are known for the rupture near the grips due to the occurring stress concentration, as stated in [32–34]. Another challenge lies in the absence of material ability to the reduction in the area during tensile testing. It is caused by a relatively small Poisson's ratio as also pointed out by De Baere et al. [32]. In order to localise the rupture in the centre of specimens, the curved configuration is thus selected. Owing to the woven composite structure, the pull-out failure might occur during testing as reported in [32], but no relationship is established between the transverse and longitudinal failures. Hence, the specimens of 0° and 90° fibre orientations are of a dumbbell-shaped geometry with the total length 250 mm, thickness 2 mm and the narrowest width 25 mm in the middle of specimens (Figure 2) containing 1.5 of RVE. Regarding the ends of the specimens, their width is restricted by the grip width and, thus, is 30 mm. The absence of the end-tabs is justified by the desiccation/absorption processes as in the case of 45° fibre-oriented specimens.

## 3 Elaboration of conditioning protocol

As already mentioned, the sensitivity of PA6 GF is caused by its chemical structure and leads to significant changes in mechanical and physical properties when exposed to thermal and hygroscopic loadings [18,23,35,36]. Hence, for a clear and consistent analysis of the mechanical behaviour, one should keep the same protocol of desiccation and absorption for all the specimens. Due to the lack of information regarding desorption/absorption procedures for this specific material, it was decided to develop such a protocol at first. It allows an accurate estimation of the time duration required to recondition specimens to a dry state, which corresponds to an environment with RH 0% theoretically and to an environment with

less than RH 10% practically. Likewise, the exposure to RH 50 % and RH 85% serves to obtain corresponding moisture contents in the specimens.

### 3.1 Desorption procedure

According to the data-sheet of PA GF, its  $T_g$  is +60°C in the dry condition. To accelerate desorption, the material should be subjected to the temperature higher than the ambient for a while [19,26]. Hence, the use of the desiccation temperature might be a sensitive issue for the mechanical material response due to varying moisture content and, thus,  $T_g$ . In order to evaluate the influence of drying temperatures on the kinetics of desorption and mechanical properties, three of them are selected: +50°C, +70°C and +90°C. Such a choice is governed and justified by  $T_g$  in the dry state. From a physical point of view, at +50°C (below  $T_g$ ) the composite is brittle and hard when desiccated, while at +70°C and +90°C (above  $T_g$ ) the matrix of the composite material is in the viscous state. For a more rapid desorption acceleration, all specimens are placed into a climatic chamber Binder VD-115 under vacuum.

The moisture content is defined by a gravimetric method (ASTM D5229), cited by numerous authors [8,10,21,26,37], due to the absence of integrated scales in the chamber. It consists of weighing specimens regularly. The precision of scales is 0.1 mg. Resulting from the comparison of the initial mass of a specimen, right before desorption, and at several time-steps, one can observe the change in mass due to the loss of moisture (Eq. 1).

$$C_{glob} = (M_t - M_0)100\%/M_0. \quad (1)$$

In Eq. 1,  $M_0$  represents the initial mass of a specimen,  $M_t$  is the mass of the specimen at a time-step  $t$  and  $C_{glob}$  is the moisture content at a time-step  $t$ . Once the moisture content reaches the plateau and stabilises, the specimen is assumed to be in the dry state. Prolonged exposure may lead to continuous material degradation [31]. However, within the framework of the current research, we assume that no chemical damage occurs due to relatively short desorption time, and  $C_{glob}$  corresponds to the value on the plateau.

Desiccated specimens subsequently undergo the controlled tension until failure on Instron 5584 testing machine at the ambient temperature (+23°C). Being resin-dominated, the fibre orientation of 45° with the geometry, depicted in Figure 1, is preferred here. The computation is detailed in section 4.3.

From the obtained results, one can notice that the rate of desorption kinetics at +50°C, +70°C and +90°C is different. During 29 days of exposure at +50°C, the loss of moisture content is 0.797% without reaching the plateau (Figure 3). Slightly higher moisture release is observed after desorption at +70°C during 14 days. The maximum studied rate takes place at +90°C with attained stabilisation within 12 days. These results are in accordance with the data of Silva et al., Starkova et al. [19,20] for a commercial polyamide and an epoxy resin, and the role of high temperature is assumed to be an activator of rapid desorption kinetics. The moisture content  $C_{glob}$  is calculated with accordance to Eq.1 using the gravimetric method.

The impact of desorption temperatures is examined by carried tensile tests of 45°-oriented composite at ambient temperature (Figure 4). From the acquired data in “true” parameters, one can see that the mechanical response of different specimens is consistent despite three different desorption temperatures. One can notice a natural dispersion of experimental results; however, no significant impact of temperatures on mechanical parameters is observed. Hence, it is assumed that the drying temperature of +90°C does not noticeably degrade the mechanical properties, while it significantly accelerates desorption kinetics. Consequently, it is decided to adopt this temperature for desorption of the studied composite. Desorption duration is chosen as 10 days for a protocol.

### 3.2 Absorption procedure

Standard environmental conditions for automobile applications, as RH 50% and 85%, also require a protocol defining duration and temperature for the absorption process. To achieve this, previously dried specimens are placed into a climatic chamber with controlled

temperature and RH (Binder KMF-115) to monitor the mass changes. The aim is to compare the absorption kinetics at different thermal loadings and to define the duration of moisture absorption until saturation in the environments RH 85% and RH 50%. The gravimetric method is also used here for data acquisition.

The uptake of moisture is firstly studied for RH 50% at 2 temperatures, +50°C and +90°C. Humid absorption at +50°C and RH 50% lasted for 54 days and 28 days at +90°C and RH 50% (Figure 5). It is important to mention that the saturation does not reach the equilibrium value at +50°C in over 50 days. In the case of +90°C, the maximum moisture content is reached in 7 days. Comparable results are presented in [19,21] for neat polyamides. As suggested by Taktak et al., Vlasveld et al. [18,21], the diffusion coefficient increases with the ageing temperature and the latter stimulates the water uptake by the matrix of the composite. Such behaviour can occur due to the increased polymer chain motion in the amorphous part of the matrix, which is in the viscous state at above +60°C. Thus, it facilitates the penetration of water molecules with the consecutive hydrogen bonding to -NH- or carbonyl groups. In order to keep the consistency of desorption/absorption kinetics and to accelerate the procedure, as also suggested by Jia et al. [17], the temperature +90°C is selected for the further ageing tests.

Analysing Figure 5, one can notice the stabilised moisture content of +90°C/RH 50% within a relatively short period (8 days); nevertheless, the absorbed moisture tends to a slight decrease if the composite is exposed to a humid and hot environment for a long time period.

For RH 85% (Figure 6) the mass is stabilised in 2.5 days, and  $C_{glob}$  remains around 1.815%. Similar results are reported by Ishisaka et al. [8] for the moisture absorption of PA6 pellets at a constant temperature of +50°C and different RH levels. Regarding the water content relation to RH of the composite PA6 GF, it is in good agreement to the experimental results of [15,18,23] for the resin PA6. In order to ensure full saturation in moisture at RH

85%, 7 days are preferred for the protocol creation. The protocol is then used for the saturation of specimens dedicated to the tensile testing campaign.

As presented in Figure 6 and in [8], the absorption rate is higher for the greater RH level. Resulting from the linear increase of the moisture uptake with the subsequent stabilisation, the material can be characterised by Fickian diffusion equation according to [26]. The results and suggestions of non-Fickian behaviour, proposed in [38] for PA6, are not in correlation with the given composite (Figure 6 and Figure 11) in terms of non-increasing moisture content after the stabilisation; however, the smooth slope at the onset of saturation reports the opposite.

### 3.3 Conditioning of 0° and 90°-oriented specimens

This section deals with the experimental confirmation of formerly developed protocol for desiccation and absorption for PA6 GF. For that, 0° and 90° fibre orientations of the composite material are tested and compared to 45° fibre orientation. The variation of geometry (Figure 1 and Figure 2) could potentially impact desorption and/or absorption kinetics.

Specimens, presented in Figure 7, are cut from the same laminate; thus, the initial state is identical. However, the loss of moisture content is similar for 0° and 90° orientations after 21 days of desiccation but exceeds the loss of 45°-oriented specimens by 21.5%. Furthermore, while moisture absorption is stabilised (Figure 8), the moisture content is higher in 0° and 90°-oriented specimens by about 7.9% as compared to 45°-oriented. Since the thickness of all the specimens remains the same (2 mm), such differences may come from the geometry, stacking sequence, fibre orientation and its content as also proposed in [37] for the carbon-epoxy composite material. More detailed analysis is, thus, necessary.

### 3.4 Cyclic conditioning

Physical reversibility of PA6 GF is an **essential** criterion in terms of applications. The theory says that if a saturated specimen is subjected to a dry environment, it should recover to **its dry state** if the material is reversible [29,30]. Then, during the subsequent exposure to the humid conditions, it should return to its saturated state. Hence, the objective of this test is to **verify** the reversibility of the composite material.

The environmental condition of RH 85% and +90°C is chosen for the cyclic absorption – desorption as the most severe. **The** specimens are initially dried and stored into a sealing bag. Desorption and absorption procedures are completed according to **the** above-described protocol. **Each cycle consists of absorption with the consequent desorption at +90°C in vacuum.**

As **one** can see from Figure 9,  $C_{glob}$  at saturation is equal to that in Figure 6 at the same conditions. However, the maximum moisture content slightly decreases with each next cycle: 1.764%, 1.728% and 1.711% respectively, thus 5.7% of decrease from 1<sup>st</sup> to 4<sup>th</sup> cycle. Regarding the minimum value of  $C_{glob}$ , it does not remain stable either: -0.058% at the end of the 1<sup>st</sup> cycle, -0.051% after the 2<sup>nd</sup> and -0.076% after the 3<sup>rd</sup> as compared to the initial dry state. The total decrease from the 1<sup>st</sup> to the 3<sup>rd</sup> cycle is 33%. The statement of reversible physical properties is not **fully** appropriate for PA6 GF unless the mechanical properties are tested. Evernden et al., Grammatikos et al. [29,39] report similar mass loss during the hygrothermal ageing. Authors relate this behaviour to the chemical decomposition, resulting in the material draining, and the matrix cracking. The latter should increase the moisture absorption capacity, which, however, is not proved in Figure 9. **As a result, an additional investigation is necessary for altering absorption – desorption.**

### **3.5 Glass transition temperature $T_g$ for a fixed RH**

The range of  $T_g$  is evaluated with Dynamic Mechanical Analysis (DMA). The moisture evaporation during these tests occurs due to high temperatures and represents a major

challenge. In order to restrain it, the specimen geometry is of 60 mm × 10 mm × 2 mm dimensions; therefore, the moisture loss is negligible with respect to test duration. The analysis is conducted for initially conditioned material to ensure three moisture contents corresponding to RH 0%, 50% and 85% environments. Specimens are tested in a bending load mode. The correspondence to the onset of the drop in the storage modulus is used to define the critical value of  $T_g$ .

Resulting from the moisture impact,  $T_g$  alters from a positive to a negative temperature (Table 1). According to DMA,  $T_g$  is about +56°C in the dry state, which is coherent to +60°C as mentioned by a supplier of the material. When the full saturation at RH 85% occurs,  $T_g$  drastically decreases to a negative temperature, which is -1°C. In the case of the standard atmospheric conditions, RH 50%,  $T_g$  is around +23°C. Similar results are also shown by numerous authors [6,8,23,24,35,40] for filled and neat PA6. The origin of such a drop of  $T_g$  is interpreted in the mentioned articles. The plasticisation effect of moisture is the main contribution resulting in the intense motion of polymer chains.

#### 4 Tensile testing

The objective of the experimental campaign is to reveal modifications in mechanical properties of the composite subjected to different climatic conditions, introduced in the form of temperature and RH. Knowing the impact of the humid environment on the mechanical properties of PA6 [8,17,26], it is essential to examine the influence of the biggest possible range of climatic conditions. However, the standard temperature for automobile industry starts from a temperature -40°C to +80°C and the standard RH is 0%, 50% and 85%. Thus, within the framework of this research, these environmental conditions are selected to provide a rich database. The global test matrix is presented in Table 2.

##### 4.1 Specimen selection

Current woven material is presented as quasi-balanced according to the supplier, so the longitudinal (warp direction) and transverse (weft direction) properties should be similar. Fibre properties are assumed to be independent of environmental conditions. Thus, only one condition of RH 50% is applied to confirm the statement at three temperatures [41]. Specimens of 45°-oriented fibres exhibit in-plane pure shear behaviour under applied tensile forces. Therefore, the mechanical properties are dominated by the matrix that is profoundly impacted by the environmental conditions.

Regarding the tensile testing of 45°-oriented specimens, 1 is monotonic till rupture and 4 undergo cyclic quasi-static loading. The sixth specimen, called here a reference specimen, is used for the evaluation of the mass change during testing. This method consists in weighing the specimen right after the bag opening, then placing it in the climatic chamber and reweighing when all 5 tests are accomplished. Such specimen is also used for experiments of 0° and 90° test batches. However, no cyclic tests are done due to the little and negligible impact of the matrix on material damage. Hence, 3 specimens of 0° and 90° fibre orientation are used for mechanical tests per condition and 1 specimen is the reference one.

#### 4.2 Testing equipment

The tests at positive temperatures are conducted on the Instron 5584 testing machine, equipped with a load cell of 150 kN and a climatic chamber with temperature regulation. For 0° and 90°-oriented specimens, data are acquired using strain gauges and images of effective length taken with a high-resolution camera via VIC-SNAP software for DIC. A speckle pattern is used to obtain the deformation field. Because of large deformations of 45°-oriented specimens, only DIC measurement is performed. Experiments at negative temperatures are carried out on the testing machine Instron 4505 with 100 kN load cell at CETIM Nantes. Due to the cold-gas circulation, taken images contain noise, thus longitudinal and transversal extensometers are used.

### 4.3 Computation procedure

The **acquired** data is used for the computation of macroscopic properties of the composite material. Regarding the mechanical properties, the in-plane shear parameters **in the local frame** are determined in “true” values, which are based on the “engineering” terms, due to large strains (Eq. 2 – 4) [42]. Clarification of in-plane shear properties is illustrated in Figure 10 on a theoretical shear stress – shear strain curve.

$$\gamma_{12 \text{ true}} = \ln(1 + \varepsilon_{xx \text{ eng}}) - \ln(1 + \varepsilon_{yy \text{ eng}}) \quad (2)$$

$$\sigma_{12 \text{ true}} = F(1 + \varepsilon_{xx \text{ eng}})^{2\nu^*} / 2S_0 \quad (3)$$

$$\nu^* = -\dot{\varepsilon}_{yy}^* / \dot{\varepsilon}_{xx}^* \quad (4)$$

The shear modulus  $G_{12}$  and the corresponding shear yield stress  $\sigma_{12 \text{ y true}}$  can be estimated with different methods. For instance, Zhou et al. [43] report using the slope at 0.5% of a maximum shear strain for the estimation of a shear modulus. Other authors, in [23], use the slope from 0% to 1% of strain for the computation of tensile modulus and up to 5% of deviation from the linear slope for the yield stress computation of the resin PA6. However, no formally stated method is given for this type of calculations for composite materials. Therefore, we selected another more reproducible approach based on a simple linear regression, where the shear modulus and the shear yield stress correspond to the maximum value of the coefficient of determination  $R^2$ , calculated from the experimental data of  $\gamma_{12 \text{ true}}$  and  $\sigma_{12 \text{ true}}$  (Eq. 5). This method ensures an identical data processing for all acquired data.

$$R^2 = \max(1 - \Sigma(y_i - f_i)^2 / \Sigma(y_i)^2) \quad (5)$$

The same methodology is applied to the computations of in-plane longitudinal and transverse tensile properties, evaluated according to the Eq. 6 – 9:

$$\varepsilon_{11 \text{ true}} = \ln(1 + \varepsilon_{xx \text{ eng}}) \quad (6)$$

$$\varepsilon_{22 \text{ true}} = \ln(1 + \varepsilon_{yy \text{ eng}}) \quad (7)$$

$$\sigma_{11 \text{ true}} = F(1 + \varepsilon_{xx \text{ eng}})^{2\nu^*} / S_0 \quad (8)$$

$$\sigma_{22 \text{ true}} = F(1 + \varepsilon_{xx \text{ eng}})^{2\nu^*} / S_0 \quad (9)$$

#### 4.4 Results and discussions

##### *Longitudinal and transverse directions*

Experimental testing demonstrates the actual fibre-dominated properties of the laminate as well as their variation as a function of hygrothermal conditions. [Figure 11](#) and [Table 3](#) depict the in-plane stress-strain results of longitudinally and transversally oriented specimens in the function of testing temperature and RH 50%. Hypothetically, the environmental temperature and the moisture content should not significantly impact the mechanical properties due to fibre domination. It is clearly visible in [Figure 11](#) that the elastic moduli remain practically unchanged at +23°C and +80°C (see also [Table 3](#)), however both  $E_{11}$  and  $E_{22}$  increase for about 29% at -40°C. A large scattering of tensile strength is caused by rupture occurred on the effective length of the specimens ([Figure 12](#) and [Figure 13](#)) and near the grips. Nevertheless, it does not modify the estimation of Young's moduli. Comparison of the warp and weft orientations ([Table 3](#)) demonstrates that the longitudinal properties are, however, slightly superior to the transversal. It can occur due to the weaving method when the transverse weft yarns are subjected to undulations in order to create a weave pattern, whereas the warp yarns remain fixed.

##### *Shear direction*

The composite is tested at varying moisture contents and temperatures with the total number of the combinations, or batches, equal to 15. The mechanical behaviour as a function of thermal loading is presented in [Figure 14](#) – [Figure 16](#), whereas the moisture contents are constant and correspond to RH 0%, 50% and 85%. [The testing temperature significantly impacts the](#) in-plane shear behaviour. The increase of the latter leads to the reduction of the shear strength and the partial growth of the shear strain within one moisture content. The most

significant changes occur at +23°C and +40°C. At +80°C, the drop in strength and the growth in strain take place with the rise of the moisture, however, at -40°C a more significant decrease of the mechanical properties is found in the current work as compared to 10% difference in [3,44] for polyamide-based glass fibre reinforced composite materials.

It is also worth mentioning that the shear strain at failure tends to decrease for RH 85% at elevated temperatures in comparison with RH 0% and RH 50%. It is supposed to occur beyond a critical value of moisture content. The same suggestion is proposed for the neat resin by Regrain, Taktak et al. [21,35], noted as a “threshold effect”.

In addition to the testing temperature, one can also observe the decrease in  $T_g$  with the rise of the RH level (Table 1). Such a connection between the environmental temperature and RH provokes a coupled problem with regard to mechanical response. Figure 17 illustrates the global state of the woven PA6 GF. Hence, the importance of the environment as one of the major parameters characterising the composite material is clearly demonstrated. One of such parameters can be introduced in the form of a temperature difference  $\Delta T$ , calculated as the testing temperature  $T$  subtracted from  $T_g$ :

$$\Delta T = T_g - T \quad (10)$$

The upper and the bottom graph parts are divided by the dashed black line matching the stress-strain curve with  $\Delta T$  being practically zero. The upper half represents the solid state (Figure 17, Figure 20) of specimens and the bottom one the viscous state (Figure 17, Figure 21) resulting from the exceeding the defined  $T_g$  (Table 1). Specific mechanical responses coincide, especially in the plastic region, even though the batches are of diverse environmental state. It can thus be justified by the adjacent values of  $\Delta T$  for pairs “testing temperature – RH”. One can suggest that as long as  $\Delta T$  is the same or close for several batches, their mechanical behaviour would be similar despite the environmental testing conditions. As a consequence, the number of required experiments for the rigorous material

examination could be significantly reduced. Nevertheless, this method does not suit some pairs with the similar values of  $\Delta T$ , for instance, the batch of  $-40^{\circ}\text{C}$  RH 85% with  $\Delta T$  of  $+39^{\circ}\text{C}$  is eventually closer to  $\Delta T$  of  $+66^{\circ}\text{C}$  and  $+63^{\circ}\text{C}$  rather than  $+33^{\circ}\text{C}$ . Similarly, the behaviour of the batch  $+80^{\circ}\text{C}$  RH 0%, so the  $\Delta T$  is  $-24^{\circ}\text{C}$ , is close to  $+40^{\circ}\text{C}$  RH 50% with  $\Delta T$   $-17^{\circ}\text{C}$  instead of  $+23^{\circ}\text{C}$  RH 85%. The authors did not find any clear explanation for such divergence. Miri et al. [45] likewise report the importance of  $\Delta T$  as a criterion for the characterisation of PA6 films; and the authors demonstrate the results that are in agreement with this study.

Figure 18 describes the pattern of modified in-plane shear modulus as a function of  $\Delta T$ . It is evident that  $G_{12}$  tends to increase with the rising value of  $\Delta T$ . This signifies that the plasticisation occurs faster in hot and humid conditions as compared to the cold and dry environment at the same strain rate. The results are consistent with the study in [21,25] on a neat PA6, who demonstrate the significant drop of tensile strength and modulus as a result of increasing water content in the material.

The in-plane shear yield stress is consistent with the shear modulus. The yield stress rises along with the increase of  $\Delta T$  (Figure 19). Consequently, the elastic domain is hardly pronounced in hot and humid conditions. It can be attributed to the fact that the polymer does not possess a distinct yield point [23]. Comparable decrease of a linear part of the “stress-strain” slopes as a function of absorbed water by PA6 and testing temperature is also reported in [23], though the moisture impact is assumed to be more severe. The authors show the modifications of the yield stress and the tensile modulus affected by testing temperature (from  $+4^{\circ}\text{C}$  to  $+80^{\circ}\text{C}$ ) and water content (from 0% to 9.3%). Equivalently, the latter has a stronger effect with the following drop of properties up to 90%. It is associated with more significant mobility of polymer chains.

Looking at the ruptured specimens, it is possible to estimate the material state *visually* – either solid (Figure 20) or viscous (Figure 21). The plastic deformation is *evident* along with the ductile rupture in the last figure when the simply elastic deformation and the brittle fracture occur in the other cases. When  $\Delta T$  is close to 0°C, a coupled problem is to appear; however, the specimens still tend to the brittle rupture rather than ductile.

Specimens of 45° stacking sequence undergo the fibre reorientation while testing (Figure 21), particularly of long duration. Such adjustment can result in miscalculated *local* mechanical parameters if the new fibre orientation is *not* taken into consideration at each time-step of a test. Hence, it is of great interest to dip into this search problem, not treated in this work.

#### *Loss/gain of moisture during testing*

The material capacity to the rapid water absorption *also* results in its relatively quick loss in uncontrolled environmental conditions [3]. In order to check the specimen desorption during the mechanical tests, each batch contains 1 reference specimen. The average testing time of a batch is around 8 hours for 45°-oriented specimens and around 2 hours for 0° and 90°-oriented specimens.

Such a method of using a reference specimen allows demonstrating the global moisture loss or gain that may occur. Nevertheless, the real moisture loss of each tested specimen does not reach the value, shown in Figure 22 and Figure 23, *because of the* relatively short test duration, whereas the reference specimen is subjected to the given environment during the *entire* batch testing. The most important mass changes occur in *the* hot atmosphere. It correlates with the desiccating procedure when the composite *is* subjected to high temperature. However, the moisture content might not be the representative parameter of the mechanical behaviour if *the* material is *in the environmental conditions that are different from studied*.

## 5 Conclusions

The presence of hygrothermal boundary conditions has a detrimental impact on the polyamide-based composite materials. In order to enrich an experimental database, the authors investigated the mechanical parameters of the woven PA6 GF under changing environment – temperature and moisture. This campaign is preceded by the protocol development aiming at ensuring required moisture content in the specimens. Hence, it is successfully employed in this work for three stacking sequences. The results of the testing campaign demonstrate a significant relation of the material state to the glass transition temperature that tends to drop when the material **absorbs the moisture**. Nevertheless, a coupled problem of “**temperature – RH**” is present. It results in the decrease of the shear modulus, shear stress at yield and, globally, in the shear stress at rupture. The shear strain is, however, increasing till a threshold, thus showing better ductile properties of the composite. The monitored mass of specimens illustrates an important material capacity to a rapid moisture loss or gain during a relatively short extent of time, **which, however**, remains in accordance with the results of desiccation/absorption protocol establishment.

**Authors do not study** the material tendency to a higher moisture loss and smaller moisture absorption during cyclic desorption/absorption testing. However, such material quality is probable to impact the physical, mechanical and properties, introducing another research and industrial significance as a long-term perspective. Mechanical response of 45° fibre-orientated specimens can also be supplemented by a varying testing velocity, thus enriching the experimental database. Regarding the short-term perspectives, the mechanical properties serve for validation of modelled RVE and numerical out-of-plane data, which are required to evaluate the composite material **thoroughly**. What is more, the obtained database demonstrates the most critical environmental conditions for the experimental campaign on

bolted joints. Hence, in terms of perspectives, the studied composite material remains of great interest and significance.

### **Acknowledgements**

This work is a part of a project guided by CETIM – GeM. The authors express their gratitude to Sophie Toillon-Rey Flandrin for the fruitful collaboration and the DMA expertise and Amélie Boisseau, Elliott Guelzec for mechanical testing at negative temperatures.

### **References**

- [1] R. Hamonou, L. Gornet, F. Jacquemin, S. Auger, Dimensionnement aux dommages des assemblages boulonnés de composites à matrice thermoplastique, in: Colloque Supméca 2015, 2015: pp. 1–10.
- [2] H. Obeid, Durabilité de composites à matrice thermoplastique sous chargement hygro-mécanique: étude multi-physique et multi-échell des relations microstructure - propriétés-états mécaniques, Thesis. Université de Nantes, 2016.
- [3] BASF Corporation, Mechanical performance of polyamides with influence of moisture and temperature – accurate evaluation and better understanding, 2003. [www.basf.com](http://www.basf.com).
- [4] J.J. Aklonis, Mechanical properties of polymers, *J. Chem. Educ.* 58 (1981) 892. doi:10.1021/ed058p892.
- [5] H.S. Choi, K.J. Ahn, J. Nam, H.J. Chun, Hygroscopic aspects of epoxy / carbon fiber composite laminates in aircraft environments, *Compos. Part A Appl. Sci. Manuf.* 32 (2001) 709–720.
- [6] A. Malpot, F. Touchard, S. Bergamo, Effect of relative humidity on mechanical properties of a woven thermoplastic composite for automotive application, *Polym. Test.* 48 (2015) 160–168. doi:10.1016/j.polymertesting.2015.10.010.
- [7] S.A. Grammatikos, M. Evernden, J. Mitchels, B. Zafari, J.T. Mottram, G.C. Papanicolaou, On the response to hygrothermal aging of pultruded FRPs used in the

- civil engineering sector, *Mater. Des.* 96 (2016) 283–295. doi:10.1016/j.matdes.2016.02.026.
- [8] A. Ishisaka, M. Kawagoe, Examination of the time-water content superposition on the dynamic viscoelasticity of moistened polyamide 6 and epoxy, *J. Appl. Polym. Sci.* 93 (2004) 560–567. doi:10.1002/app.20465.
- [9] H.W. Starkweather, The sorption of water by nylons, *J. Appl. Polym. Sci.* 2 (1959) 129–133. doi:10.1002/app.1959.070020501.
- [10] Y. Wei, N. Silikas, Z. Zhang, D.C. Watts, The relationship between cyclic hygroscopic dimensional changes and water sorption/desorption of self-adhering and new resin-matrix composites, *Dent. Mater.* 29 (2013) 218–226. doi:10.1016/j.dental.2010.10.015.
- [11] M. Broudin, P.Y. Le Gac, V. Le Saux, C. Champy, G. Robert, P. Charrier, Y. Marco, Water diffusivity in PA66: Experimental characterization and modeling based on free volume theory, *Eur. Polym. J.* 67 (2015) 326–334. doi:10.1016/j.eurpolymj.2015.04.015.
- [12] G. Youssef, S. Fréour, F. Jacquemin, Effects of moisture-dependent properties of constituents on the hygroscopic stresses in composite structures, *Mech. Compos. Mater.* 45 (2009) 369–380. doi:10.1007/s11029-009-9098-1.
- [13] G. Youssef, S. Fréour, F. Jacquemin, Stress-dependent Moisture Diffusion in Composite Materials, *J. Compos. Mater.* 43 (2009) 1621–1637. doi:10.1177/0021998309339222.
- [14] J. Fajoui, M. Mulle, S. Freour, F. Jacquemin, F. Collombet, Etude numérique de la diffusion d’humidité dans les matériaux composites instrumentés par des fibres optiques à réseaux de Bragg Numerical study of moisture diffusion in composites instrumented by optical fiber Bragg gratings, in: *JNC 17, Poitiers, 2011*: pp. 1–9.
- [15] K. Kawasaki, S. Yoshiyasu, K. Kyoichi, The extension of Nylon 6 as a function of the

- extent and nature of sorbed water, *J. Colloid Sci.* 871 (1962) 865–871.
- [16] I. Pivdiablyk, P. Rozycki, L. Gornet, F. Jacquemin, S. Auger, E.C. De Nantes, Behaviour of Bolted Composite Joints in Hygro-Thermal Environments, in: 18th European Conference on Composite Materials, Athens, 2018: pp. 24–28.
- [17] N. Jia, V.A. Kagan, Mechanical Performance of Polyamides with Influence of Moisture and Temperature – Accurate Evaluation and Better Understanding, *Plast. Fail. Anal. Prev.* (2001) 95–104.
- [18] D.P.N. Vlasveld, J. Groenewold, H.E.N. Bersee, S.J. Picken, Moisture absorption in polyamide-6 silicate nanocomposites and its influence on the mechanical properties, *Polymer (Guildf)*. 46 (2005) 12567–12576. doi:10.1016/j.polymer.2005.10.096.
- [19] L. Silva, S. Tognana, W. Salgueiro, Study of the water absorption and its influence on the Young's modulus in a commercial polyamide, *Polym. Test.* 32 (2013) 158–164. doi:10.1016/j.polymertesting.2012.10.003.
- [20] Starkova O., S. Chandrasekaran, T. Schnoor, A. Aniskevich, S. K., Relaxation-driven water diffusion in epoxy resin filled with various carbon nanoparticles, in: 18th European Conference on Composite Materials, Athens, 2018: p. 8.
- [21] R. Taktak, N. Guermazi, J. Derbeli, N. Haddar, Effect of hygrothermal aging on the mechanical properties and ductile fracture of polyamide 6: Experimental and numerical approaches, *Eng. Fract. Mech.* 148 (2015) 122–133. doi:10.1016/j.engfracmech.2015.09.001.
- [22] I.F. Kaimin, A.P. Apinis, Y.Y. Galvanovskii, The effect of the moisture content on the transition temperatures of polycapramide, *Vysok. Soyed. A17* (1975) 41–45.
- [23] P.-Y. Le Gac, M. Arhant, M. Le Gall, P. Davies, Yield stress changes induced by water in polyamide 6: Characterization and modeling, *Polym. Degrad. Stab.* 137 (2017) 272–280. doi:10.1016/j.polymdegradstab.2017.02.003.

- [24] K.P. Pramoda, T. Liu, Effect of moisture on the dynamic mechanical relaxation of polyamide-6/clay nanocomposites, *J. Polym. Sci. Part B Polym. Phys.* 42 (2004) 1823–1830. doi:10.1002/polb.20061.
- [25] H.K. Reimschuessel, Relationships on the effect of water on glass transition temperature and Young's modulus of Nylon 6, *J. Polym. Sci. Polym. Chemisrty Ed.* 16 (1978) 1229–1236. doi:10. 1002/pol. 1978.170160606.
- [26] H. Obeid, A. Clément, S. Fréour, F. Jacquemin, P. Casari, On the identification of the coefficient of moisture expansion of polyamide-6: Accounting differential swelling strains and plasticization, *Mech. Mater.* 118 (2018) 1–10. doi:10.1016/j.mechmat.2017.12.002.
- [27] P. Rozycki, M.A. Mbacke, A.T. Dau, Multiscale Homogenization of a Glass-Pa66 Fabric Composite Behavior for Crash Studies, in: 18th European Conference on Composite Materials, Athens, 2018: pp. 24–28.
- [28] J.S. Lyons, Time and Temperature Effects on the Mechanical Properties of Glass-Filled Amide-Based Thermoplastics, *Polym. Test.* 17 (1998) 237–245.
- [29] M. Evernden, S. Grammatikos, S. Papatzani, U. Kingdom, Investigating the Reversibility of Moisture Uptake on the Behavior of a Pultruded Polymer Composite Used in Construction, in: 18th European Conference on Composite Materials, Athens, 2018: pp. 24–28.
- [30] O. Starkova, S. Chandrasekaran, L.A.S.A. Prado, F. Tölle, R. Mülhaupt, K. Schulte, Hydrothermally resistant thermally reduced graphene oxide and multi-wall carbon nanotube based epoxy nanocomposites., *Polym. Degrad. Stab.* 98 (2013) 519–526.
- [31] R. Bernstein, K.T. Gillen, Nylon 6.6 accelerating aging studies: II. Long-term thermal-oxidative and hydrolysis results, *Polym. Degrad. Stab.* 95 (2010) 1471–1479. doi:10.1016/j.polymdegradstab.2010.06.018.

- [32] I. De Baere, W. Van Paepegem, C. Hochard, J. Degrieck, On the tension-tension fatigue behaviour of a carbon reinforced thermoplastic part II: Evaluation of a dumbbell-shaped specimen, *Polym. Test.* 30 (2011) 663–672. doi:10.1016/j.polymertesting.2011.05.005.
- [33] I. De Baere, W. Van Paepegem, J. Degrieck, On the Design of End Tabs for Quasi-Static and Fatigue Testing of Fibre-Reinforced Composites, *Polym. Compos.* 10 (2009) 381–390. doi:10.1002/pc.
- [34] V.L. Kulakov, Y.M. Tarnopol'skii, A.K. Arnautov, J. Rytter, Stress-strain state in the zone of load transfer in a composite specimen under uniaxial tension, *Mech. Compos. Mater.* 40 (2004) 91–100. doi:10.1023/B:MOCM.0000025483.37317.e2.
- [35] C. Regrain, Comportement, endommagement et fissuration par fluage du Polyamide 6 : étude expérimentale et modélisation, Ecole Nationale Supérieure des Mines de Paris, 2009.
- [36] D.P.N. Vlasveld, M. De Jong, H.E.N. Bersee, A.D. Gotsis, S.J. Picken, The relation between rheological and mechanical properties of PA6 nano- and micro-composites, *Polymer (Guildf)*. 46 (2005) 10279–10289. doi:10.1016/j.polymer.2005.08.002.
- [37] J. Jedidi, Contribution à la Caractérisation en Cyclage Hygrothermique d'un Matériau Composite. Application à l'Avion Supersonique, Thesis. Ecole Nationale Supérieure des Mines, 2005.
- [38] M. Arhant, P.Y. Le Gac, M. Le Gall, C. Burtin, C. Briançon, P. Davies, Modelling the non Fickian water absorption in polyamide 6, *Polym. Degrad. Stab.* 133 (2016) 404–412. doi:10.1016/j.polymdegradstab.2016.09.001.
- [39] S.A. Grammatikos, R.J. Ball, M. Evernden, R.G. Jones, Impedance spectroscopy as a tool for moisture uptake monitoring in construction composites during service, *Compos. Part A Appl. Sci. Manuf.* 105 (2018) 108–117.

doi:10.1016/j.compositesa.2017.11.006.

- [40] A. Launay, Y. Marco, M.H. Maitournam, I. Raoult, Modelling the influence of temperature and relative humidity on the time-dependent mechanical behaviour of a short glass fibre reinforced polyamide, *Mech. Mater.* 56 (2013) 1–10. doi:10.1016/j.mechmat.2012.08.008.
- [41] M. Loos, *Carbon Nanotube Reinforced Composites: CNT Polymer Science and Technology*, Elsevier, 2015.
- [42] J. Lemaitre, J.-L. Chaboche, A. Benallal, R. Desmorat, *Mécanique des matériaux solides*, 3rd ed., Dunod, 2009.
- [43] G. Zhou, E.R. Green, C. Morrison, In-plane and interlaminar shear properties of carbon/epoxy laminates, *Compos. Sci. Technol.* 55 (1995) 187–193. doi:10.1016/0266-3538(95)00100-X.
- [44] BASF Corporation, An advanced high modulus (HMG) short glass-fiber reinforced Nylon 6: Part I - Role and kinetic of fiber-glass reinforcements, 2003. [www.basf.com](http://www.basf.com).
- [45] V. Miri, O. Persyn, J.M. Lefebvre, R. Seguela, Effect of water absorption on the plastic deformation behavior of nylon 6, *Eur. Polym. J.* 45 (2009) 757–762. doi:10.1016/j.eurpolymj.2008.12.008.

Figure 1 Specimen geometry of 45° fibre orientation

Figure 2 Specimen geometry of 0° and 90° fibre orientations

Figure 3 Desorption of PA6 GF at 50°C, 70°C and 90°C in vacuum

Figure 4 Tensile tests of PA6 GF specimens at ambient temperature after desiccation at three temperatures

Figure 5 Comparison of humid ageing at +50°C and +90°C

Figure 6 Moisture absorption of PA6 GF at 90°C and RH 50%/RH 85%

Figure 7 Desorption procedure of specimens with differently oriented fibres

Figure 8 Moisture absorption of 0°, 90° and 45°-oriented composites at RH 50% and 90°C

Figure 9 Cyclic absorption/desorption: RH 0% ↔ RH 85%

Figure 10 Theoretical shear stress – shear strain curve with utilised notation

Figure 11 Stress-strain response of PA6 GF, oriented at 0° and 90°

Figure 12 Ruptured specimens of 90° orientation at -40°C and RH 50%. Non-broken specimen is the reference

Figure 13 Ruptured specimens of 0° orientation at +80°C and RH 50%. Non-broken specimen is the reference

Figure 14 Stress-strain response of PA6 GF at RH 0%

Figure 15 Stress-strain response of PA6 GF at RH 50%

Figure 16 Stress-strain response of PA6 GF at RH 85%

Figure 17 Reassembled shear stress-strain curves

Figure 18 Shear modulus as a function of  $\Delta T$

Figure 19 Shear stress at yield point as a function of  $\Delta T$

Figure 20 Ruptured specimens of 45° orientation at -40°C and RH 0%. Non-broken specimen is the reference.  $\Delta T$  is -96°C

Figure 21 Ruptured specimens of 45° orientation at +80°C and RH 85%. Non-broken specimen is the reference.  $\Delta T$  is +81°C

Figure 221 Loss in mass of reference specimens of PA6 GF oriented at 45°

Figure 23 Loss in mass of reference specimens of PA6 GF at RH 50% oriented at 0° and 90°

	<i>RH 0%</i>	<i>RH 50%</i>	<i>RH 85%</i>	Type of analysis	Specimen
Glass transition temperature	+56°C	+23°C	-1°C	DMA Bending mode	60 mm × 10 mm × 2 mm

Table 1 Glass transition temperature for different moisture contents

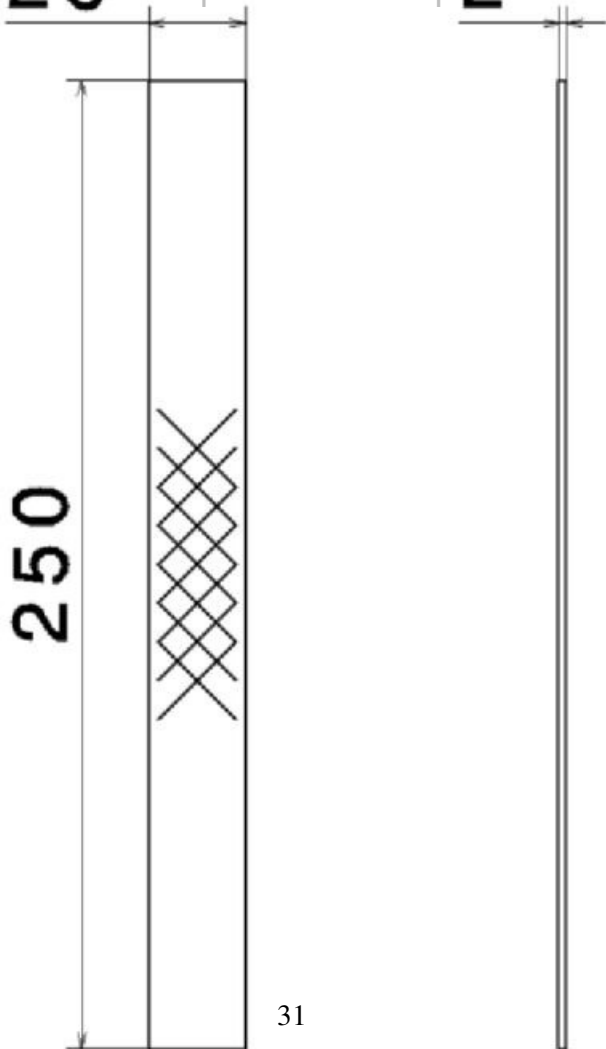
	<b>RH 0%</b>	<b>RH 50%</b>	<b>RH 85%</b>
<b>-40°C</b>	45°	45° 0° 90°	45°
<b>-10°C</b>	45°		45°
<b>+23°C</b>	45°	45° 0° 90°	45°
<b>+40°C</b>	45°		45°
<b>+80°C</b>	45°	45° 0° 90°	45°

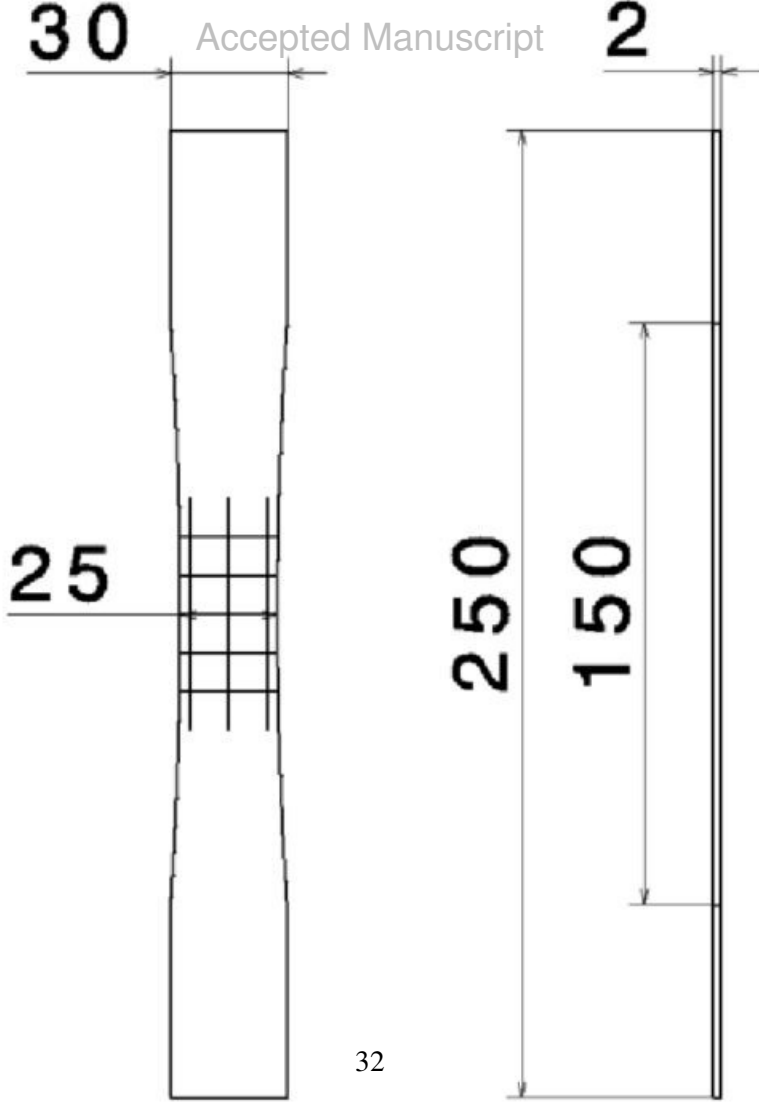
where 45°, 0°, 90° are the fibre orientations

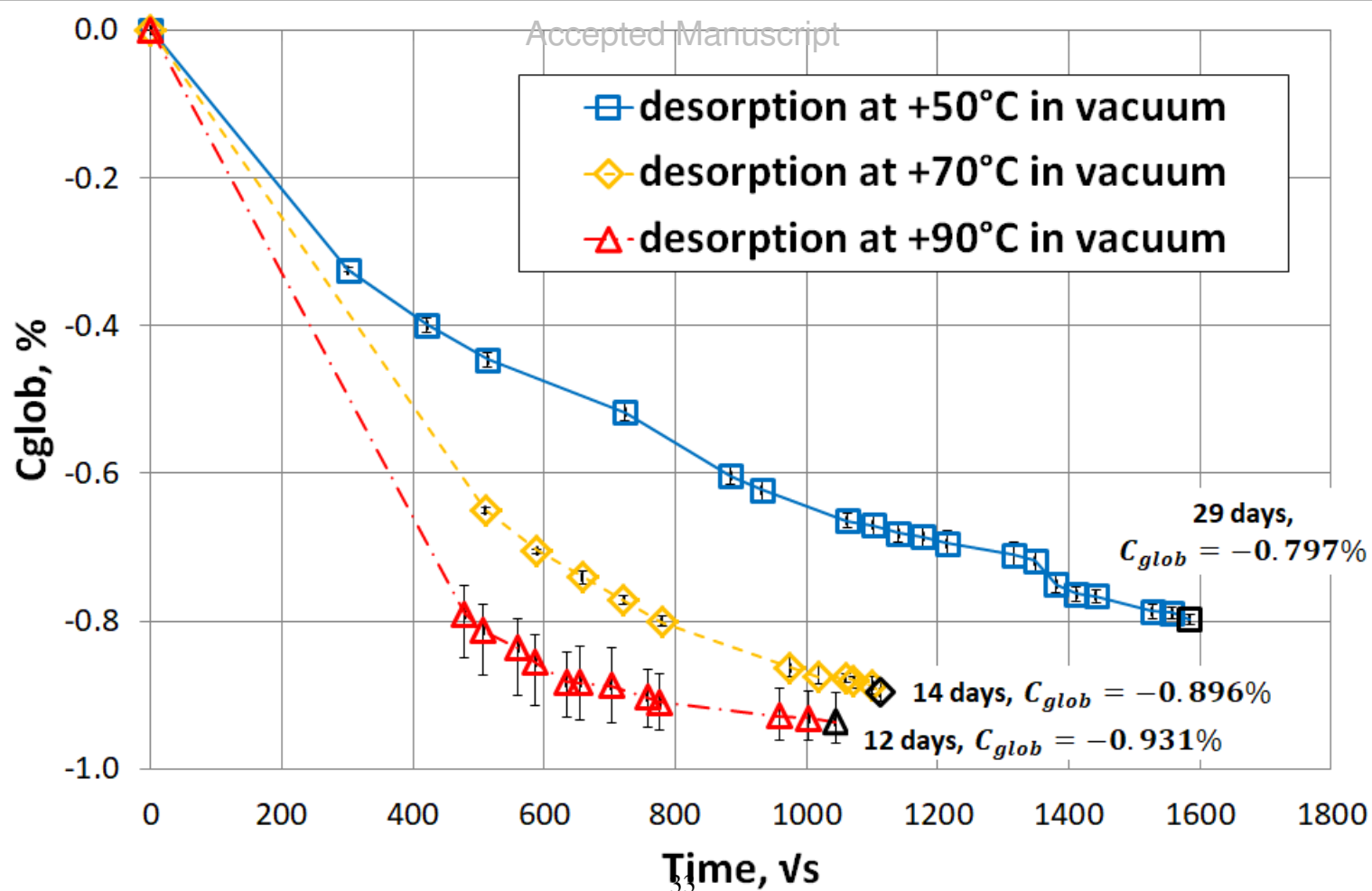
Table 2 Test matrix

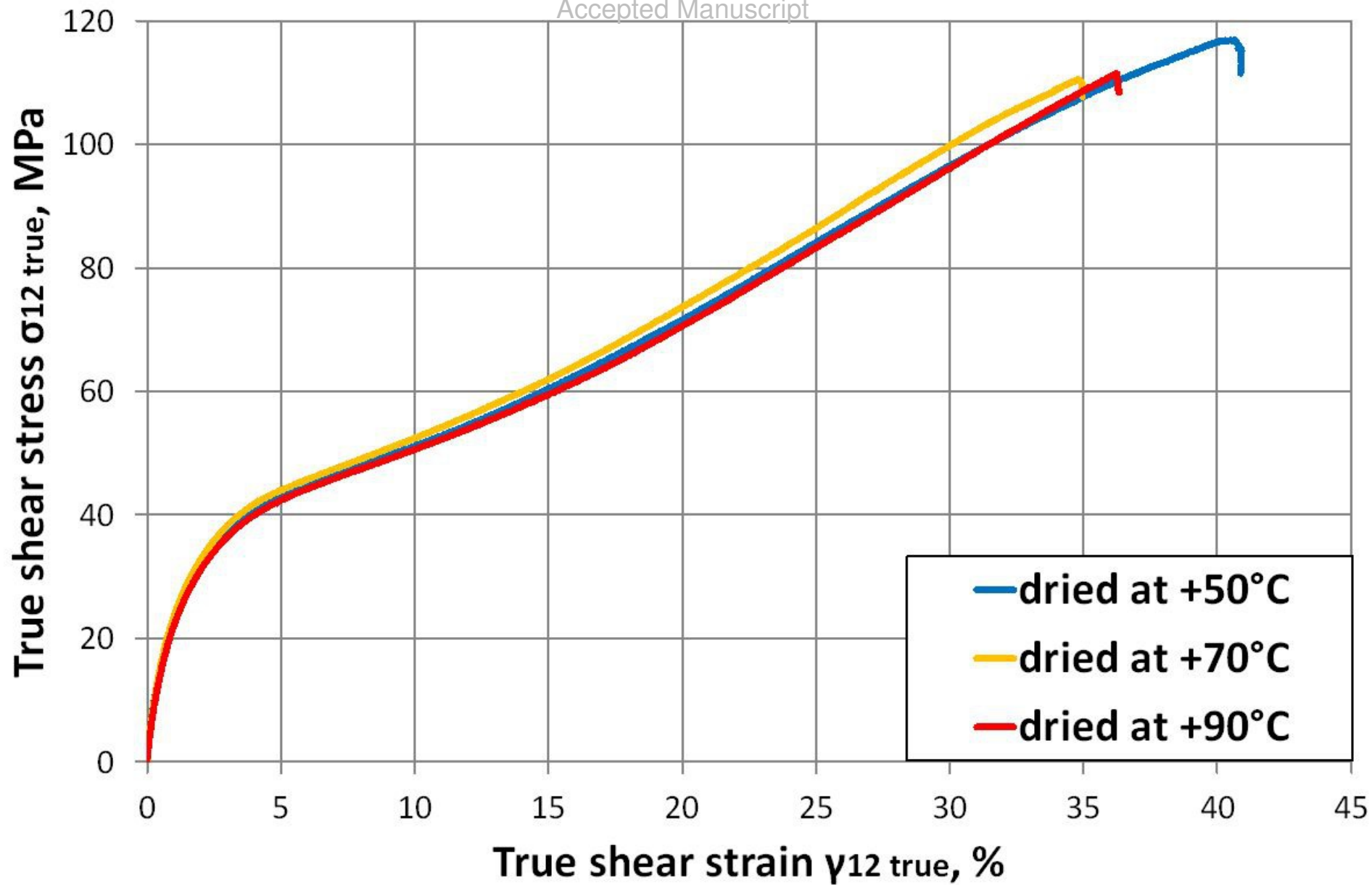
RH	Temp	45°				0°			90°		
		$G_{12}$ MPa	$\sigma_{12}$ <i>true</i> MPa	$\sigma_{12}$ <i>true max</i> MPa	$\gamma_{12}$ <i>true max</i> %	$E_{11}$ MPa	$\sigma_{11}$ <i>true max</i> MPa	$\nu_{12}$ (-)	$E_{22}$ MPa	$\sigma_{22}$ <i>true max</i> MPa	$\nu_{21}$ (-)
0%	-40°C	4768.59 ±119.35	6.53 ±0.68	151.20 ±5.91	32.34 ±2.14	-	-	-	-	-	-
	-10°C	4350.45 ±162.85	6.46 ±0.73	130.92 ±8.15	33.29 ±0.44	-	-	-	-	-	-
	+23°C	3843.20 ±157.19	6.17 ±1.16	125.57 ±3.59	41.37 ±5.47	-	-	-	-	-	-
	+40°C	3527.23 ±574.69	6.06 ±3.52	114.41 ±9.31	43.05 ±3.84	-	-	-	-	-	-
	+80°C	1223.31 ±109.24	2.82 ±0.16	116.56 ±7.42	65.31 ±7.15	-	-	-	-	-	-
50%	-40°C	5070.88 ±320.79	6.79 ±1.22	111.30 ±6.93	26.80 ±2.72	27909.5 ±1323.7	31.62 ±21.09	-	26029.3 ±1031.8	41.55 ±27.28	-
	-10°C	4128.48 ±110.96	5.63 ±0.35	104.58 ±2.56	33.46 ±1.45	-	-	-	-	-	-
	+23°C	2382.09 ±444.65	3.65 ±1.27	103.96 ±2.79	52.13 ±2.91	26987.1 ±2953.4	29.15 ±4.75	0.24 ±0.02	32057.2 ±3957.1	33.22 ±24.93	0.39 ±0.01
	+40°C	1749.85 ±40.20	3.34 ±0.23	96.85 ±7.06	55.83 ±5.41	-	-	-	-	-	-
	+80°C	877.54 ±166.77	3.45 ±1.69	95.53 ±1.95	66.69 ±2.00	24663.6 ±3238.9	44.56 ±15.35	0.24 ±0.07	25983.4 ±2148.3	43.86 ±42.99	0.26 ±0.09
85%	-40°C	5054.76 ±159.19	7.71 ±3.44	112.71 ±9.03	30.44 ±3.88	-	-	-	-	-	-
	-10°C	3079.09 ±991.49	6.57 ±2.18	93.91 ±2.59	35.54 ±1.81	-	-	-	-	-	-
	+23°C	1332.19 ±92.65	2.90 ±0.28	86.88 ±7.65	54.63 ±8.87	-	-	-	-	-	-
	+40°C	1252.59 ±253.45	2.44 ±0.24	80.29 ±9.19	53.93 ±5.93	-	-	-	-	-	-
	+80°C	721.92 ±151.19	3.87 ±2.79	74.27 ±5.86	58.94 ±4.83	-	-	-	-	-	-

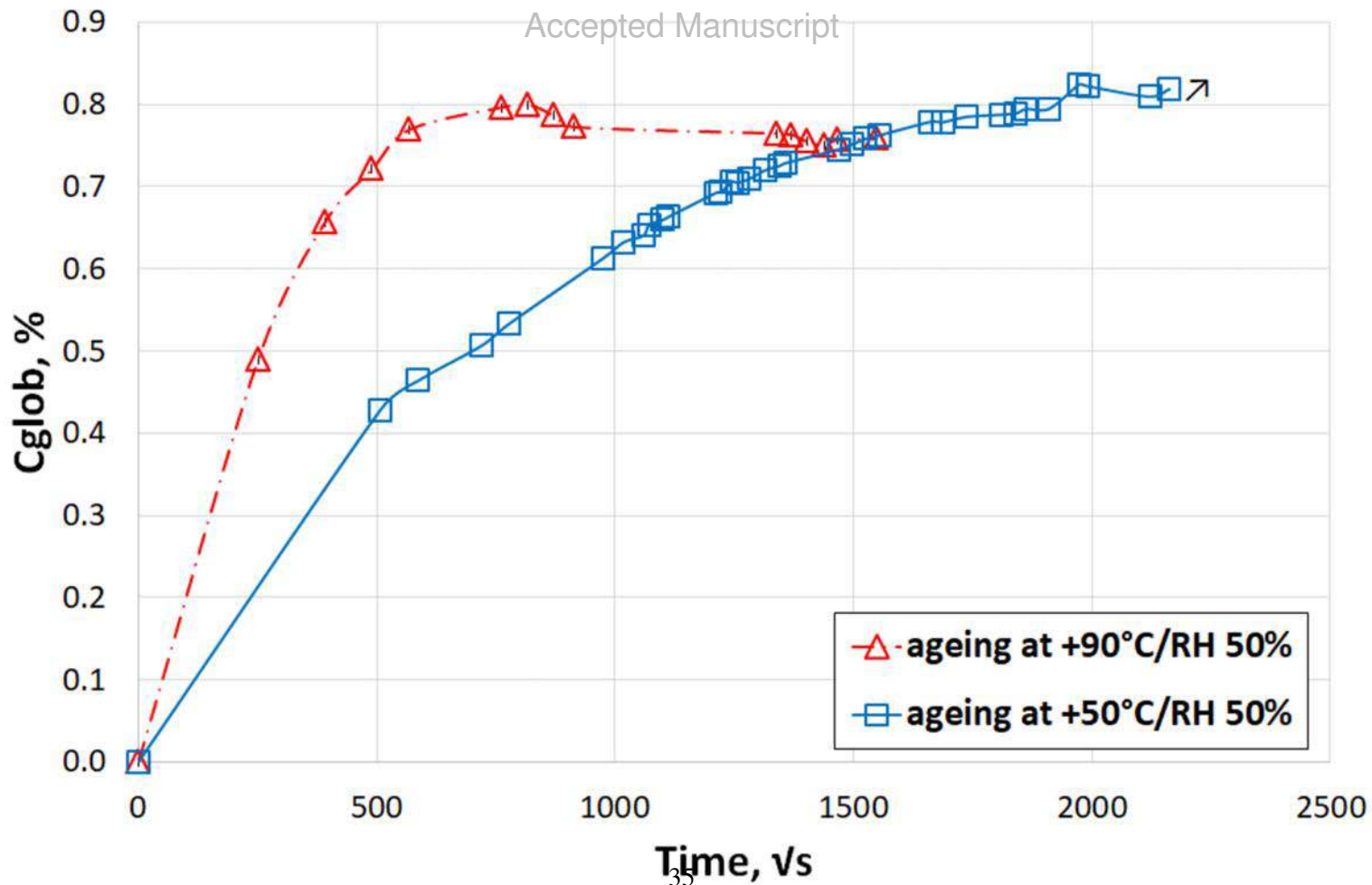
Table 3 Mechanical properties of PA6 GF subjected to humidity and temperature

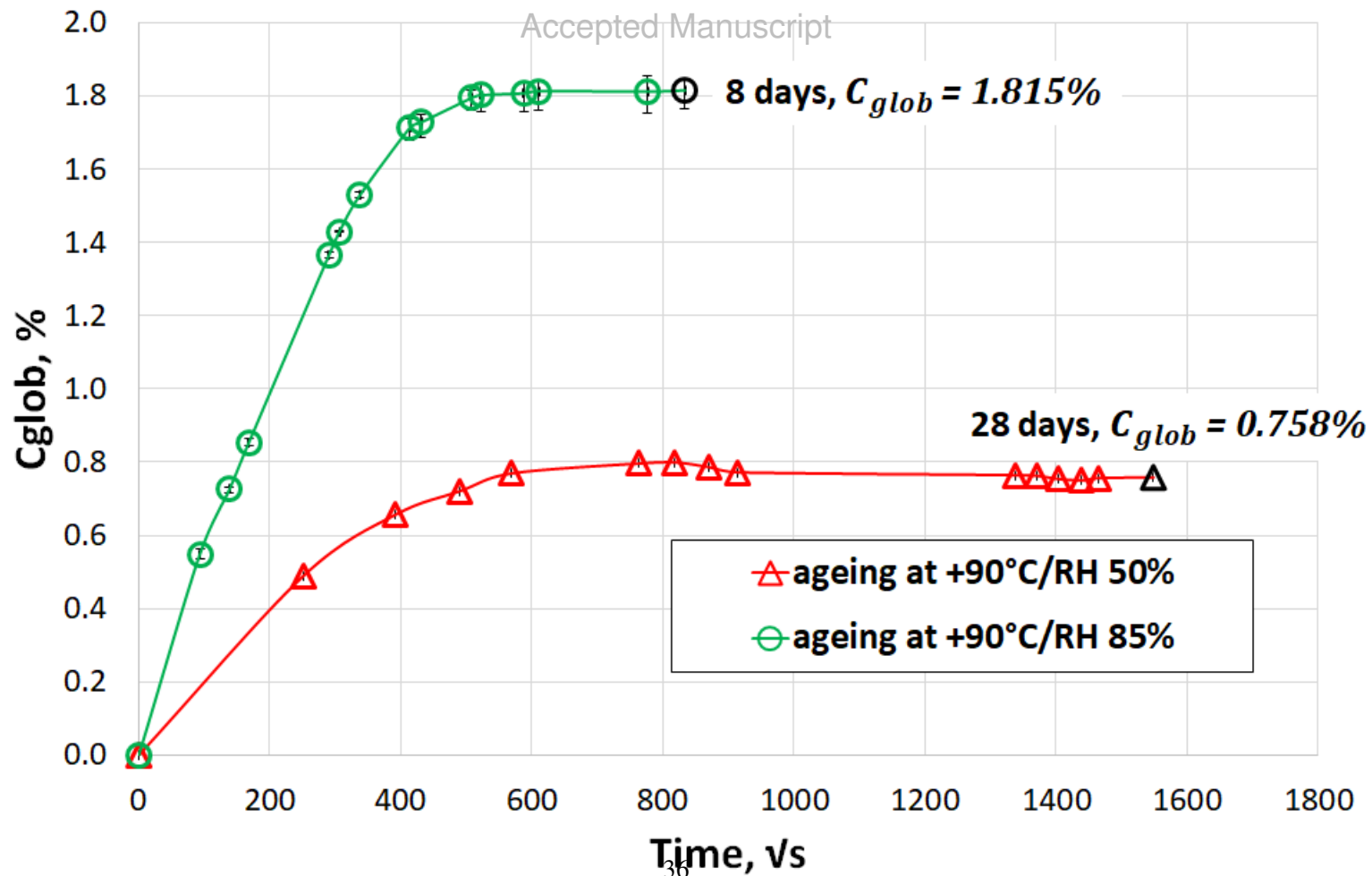


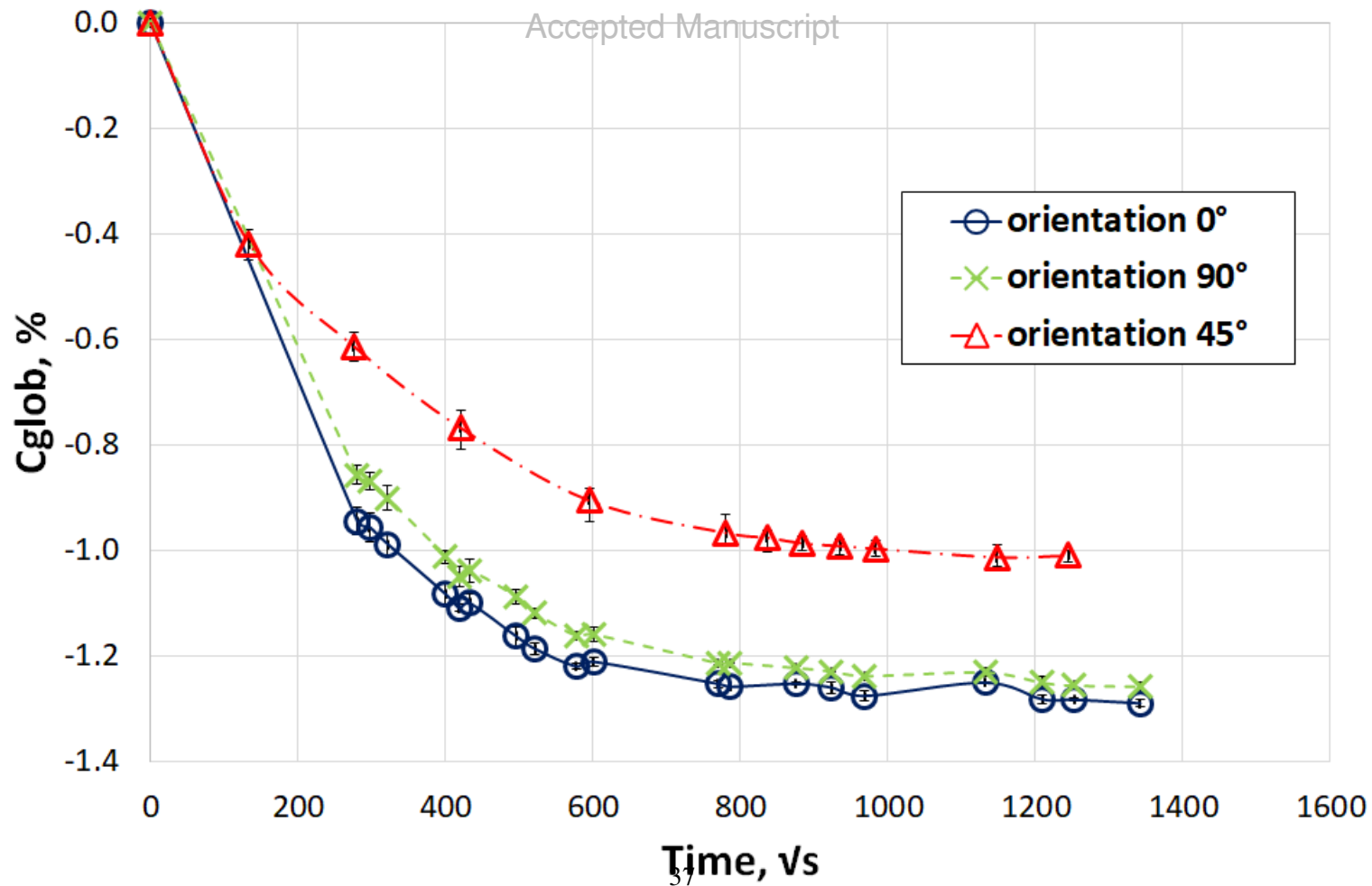


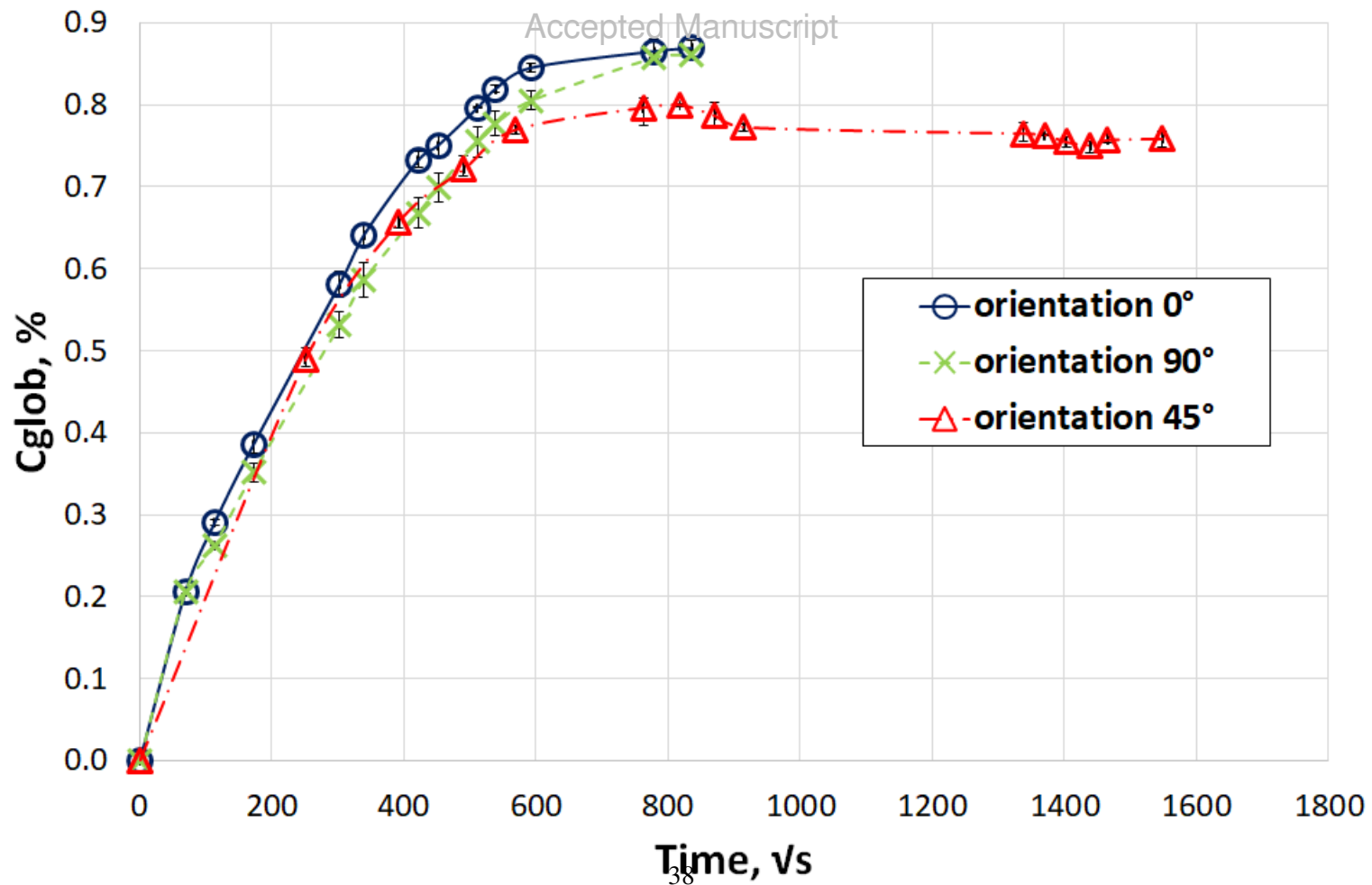


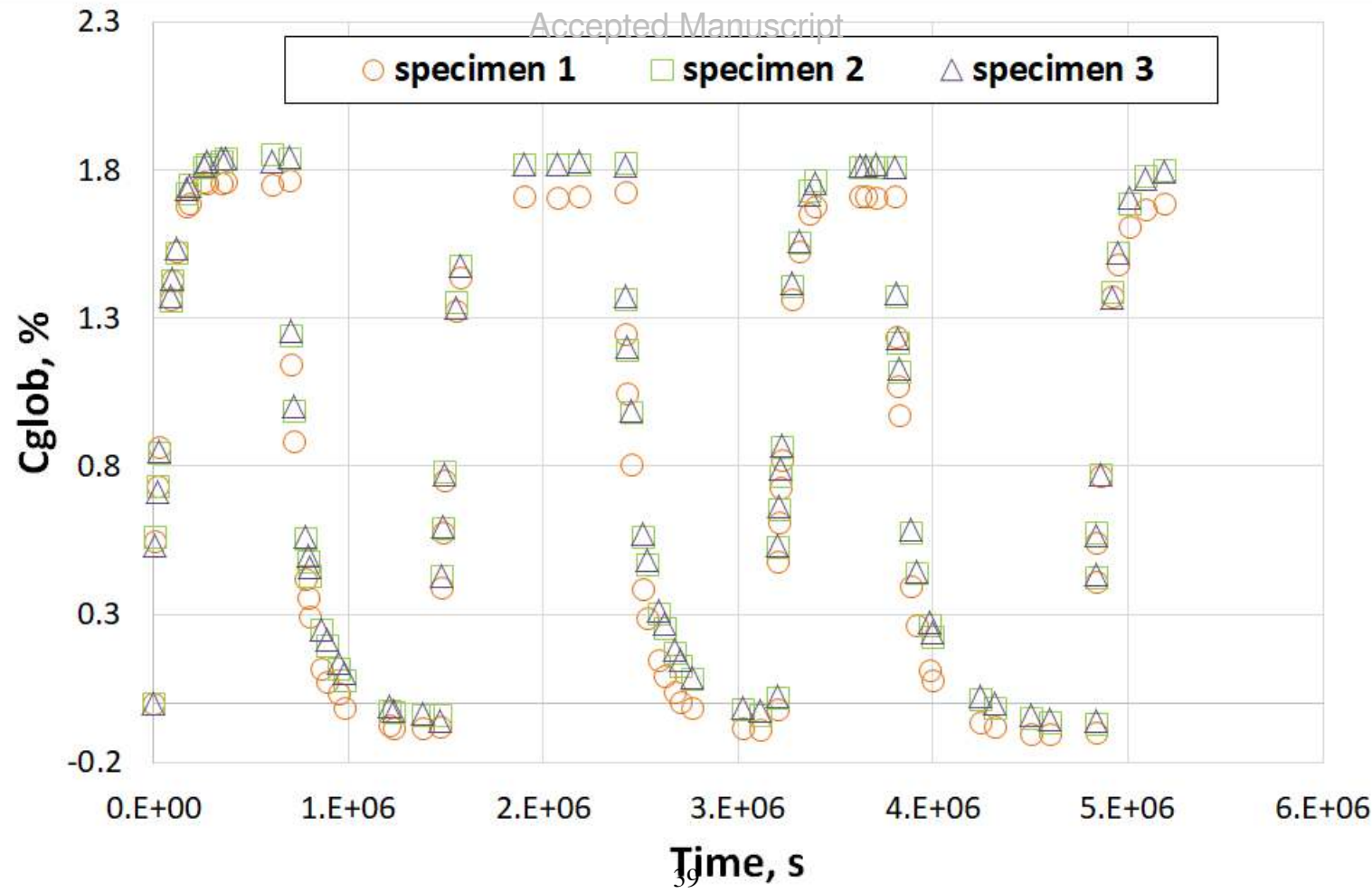


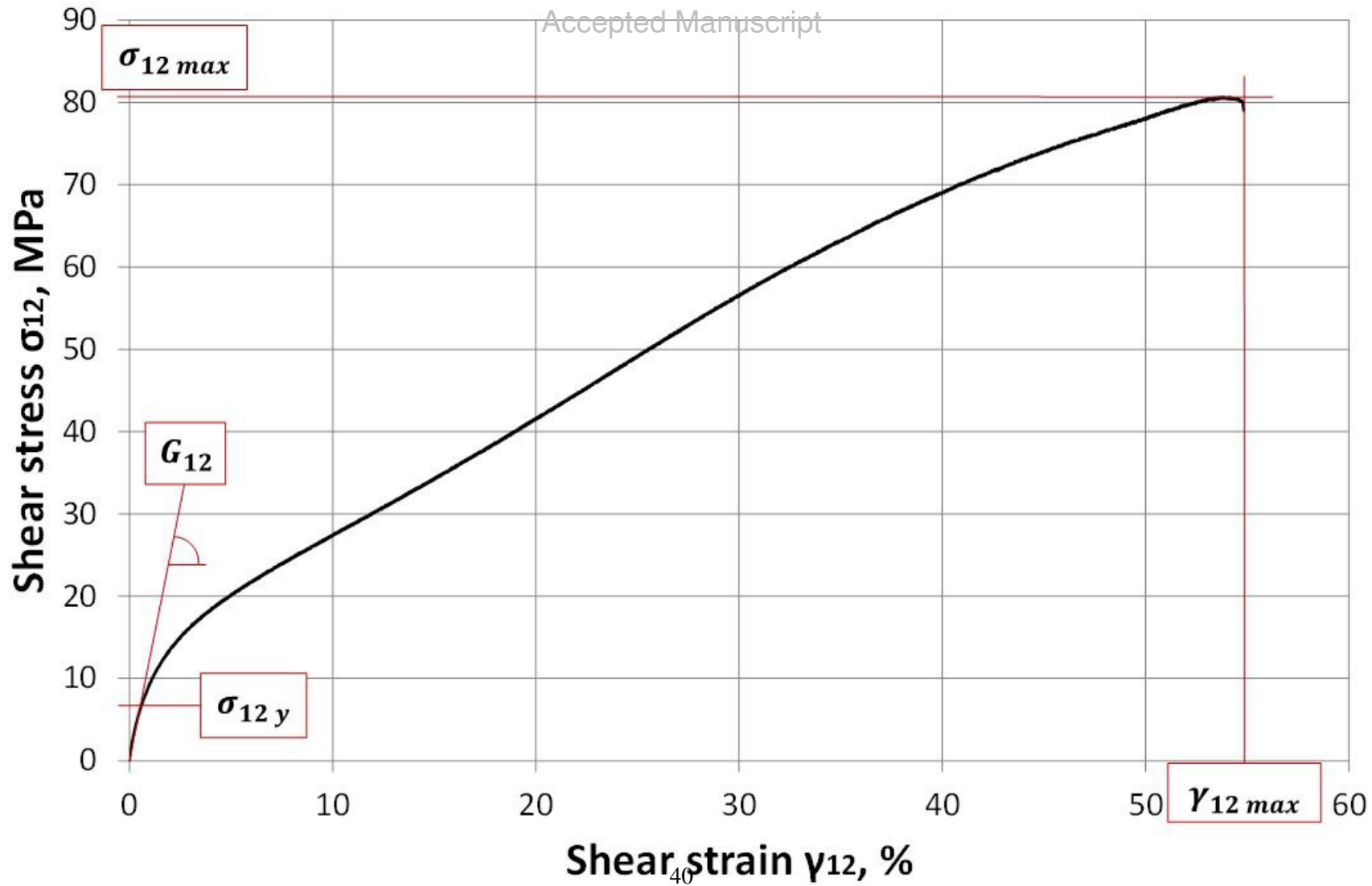


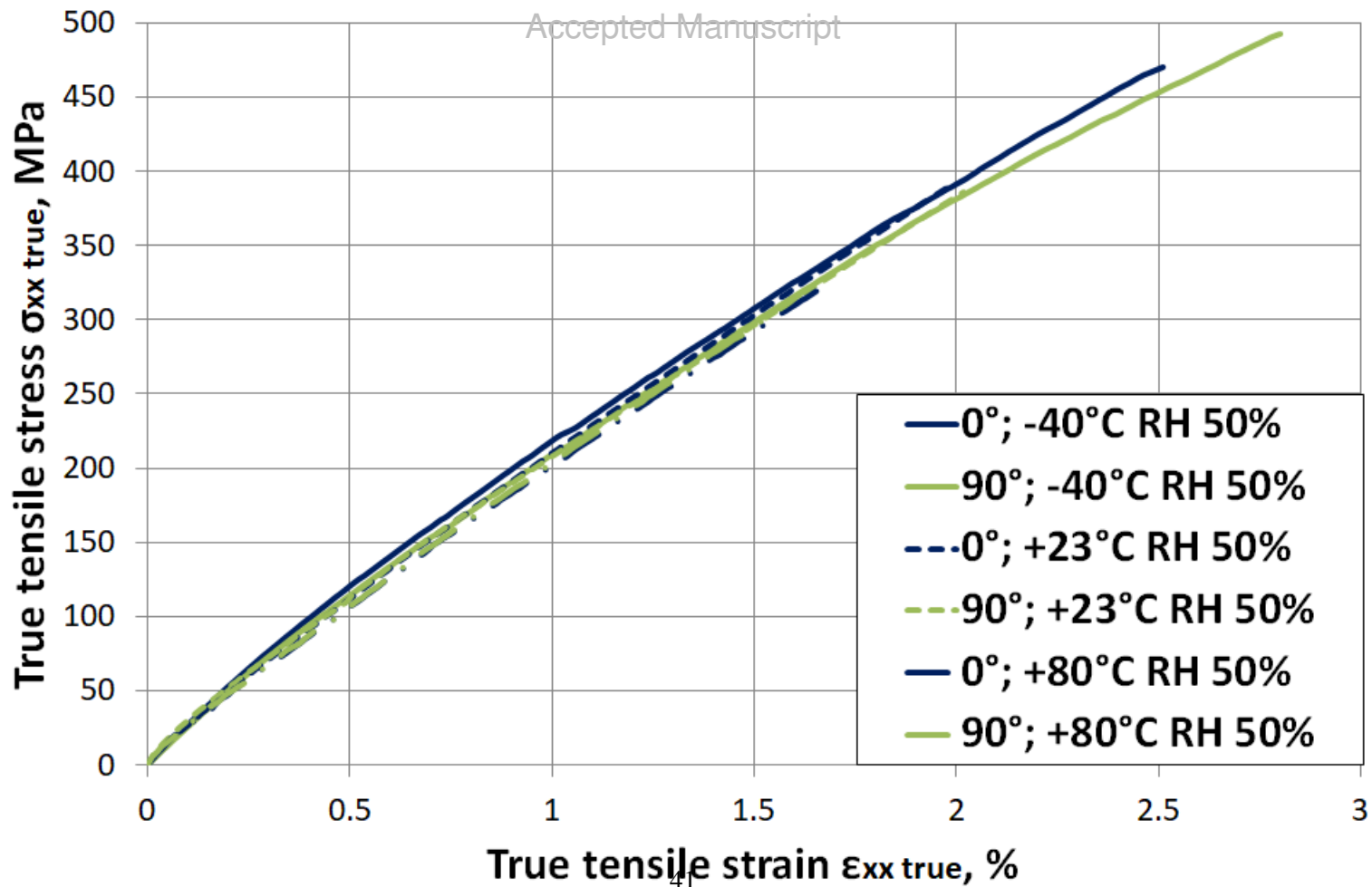












90 3 3

90 2 2

90 1 1

10/HR50  
L96J  
S  
X  
25°C

0

3

0

2

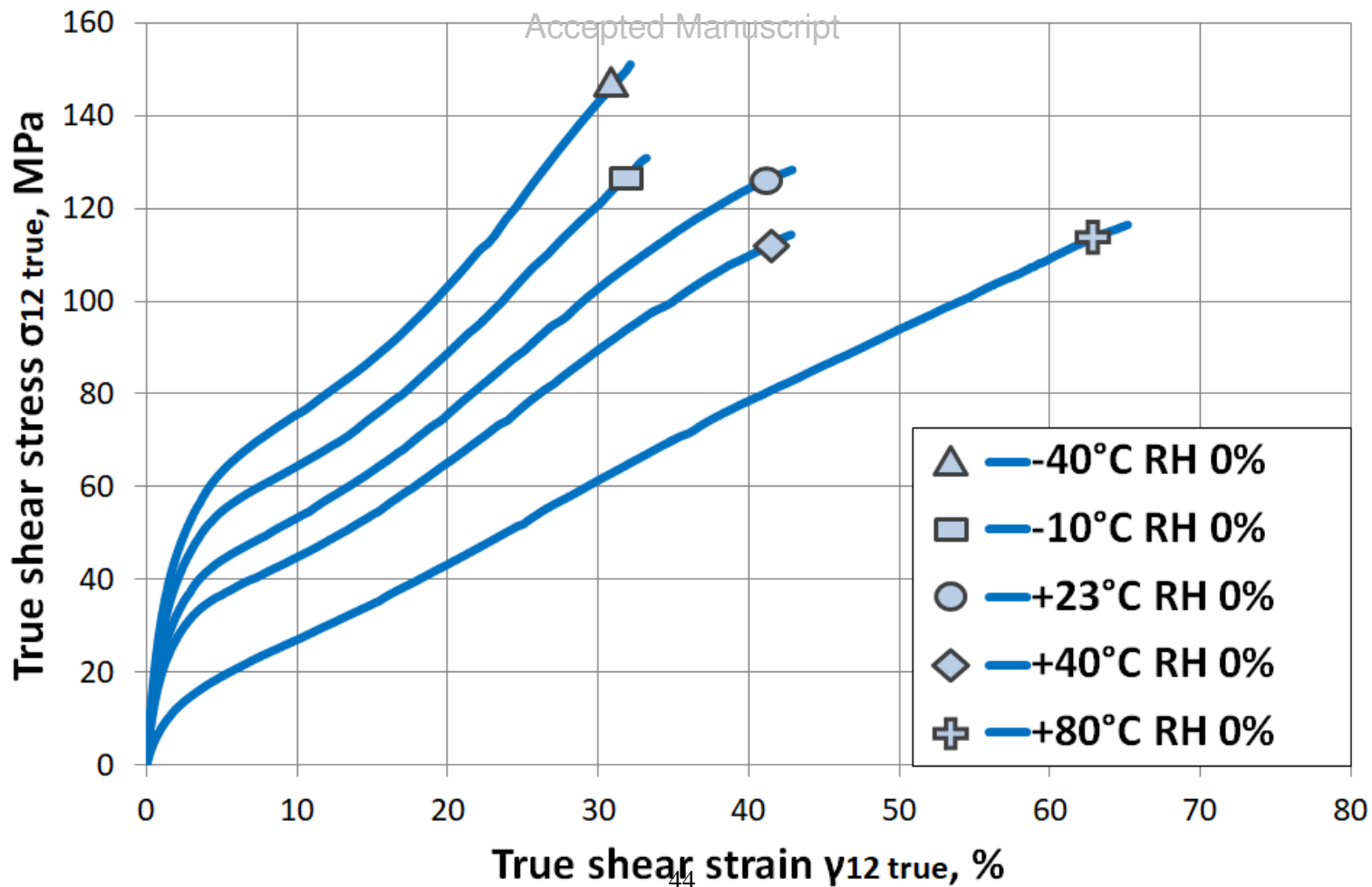
0

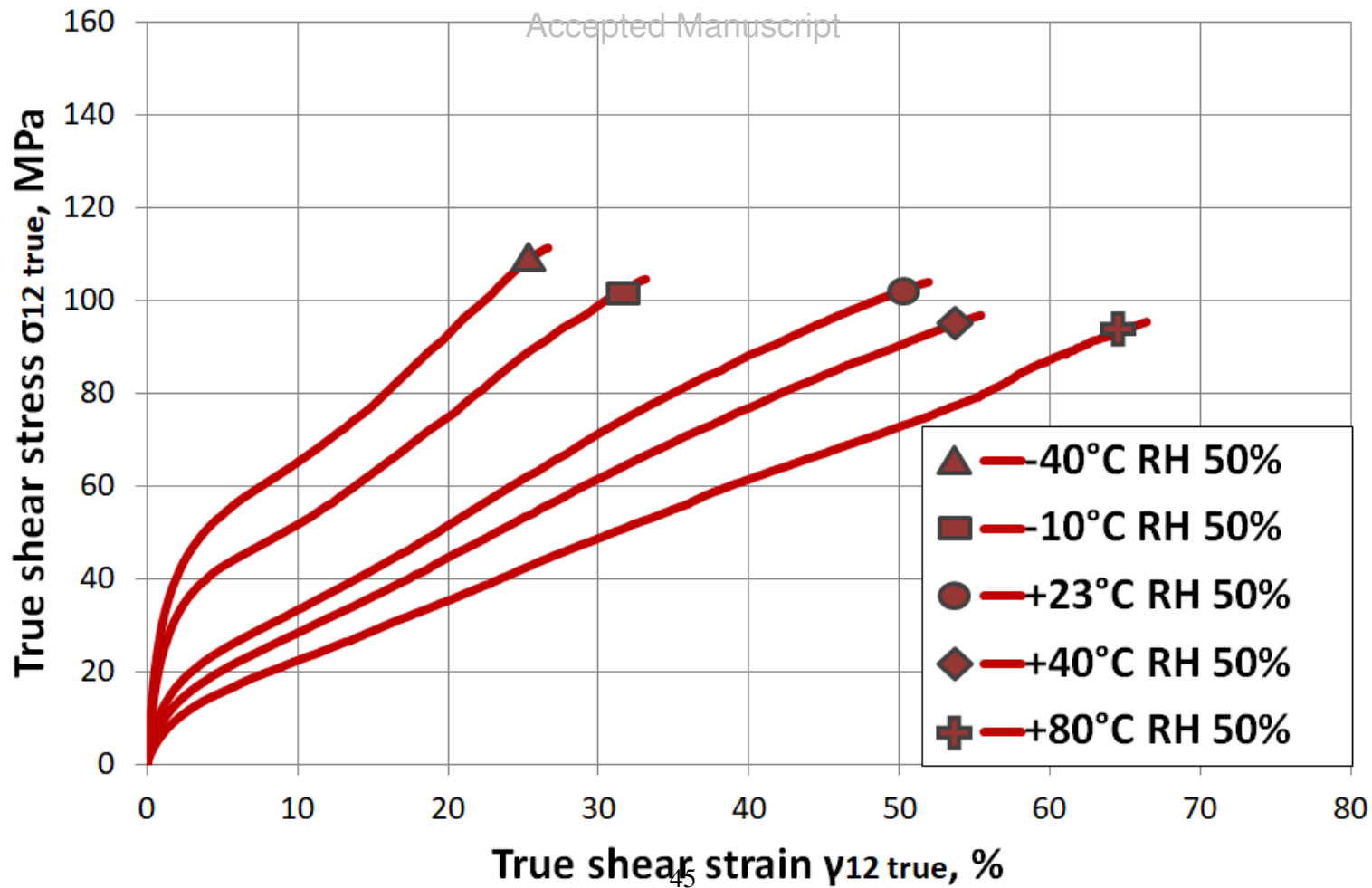
1

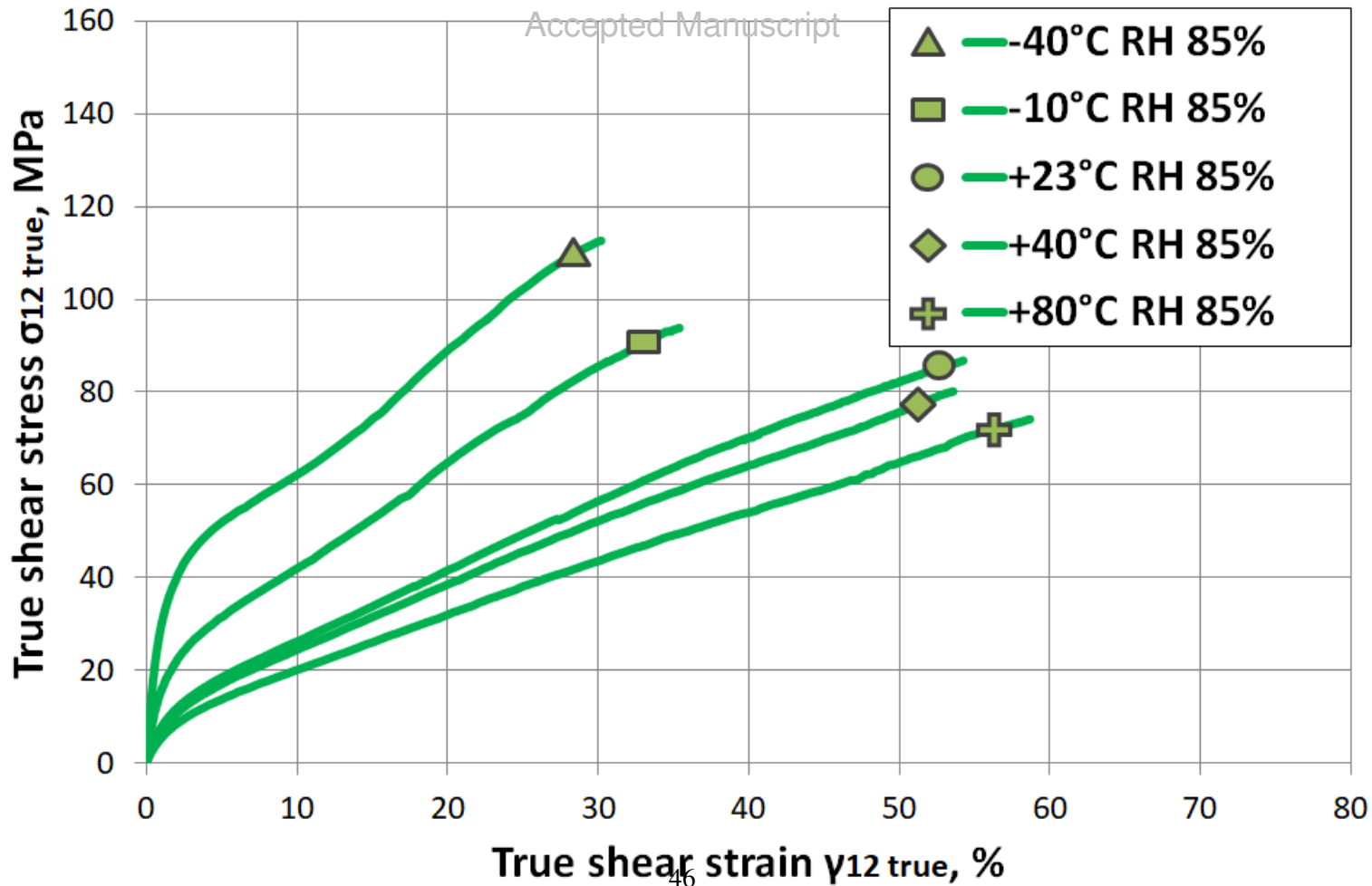
6/50MR  
107  
S

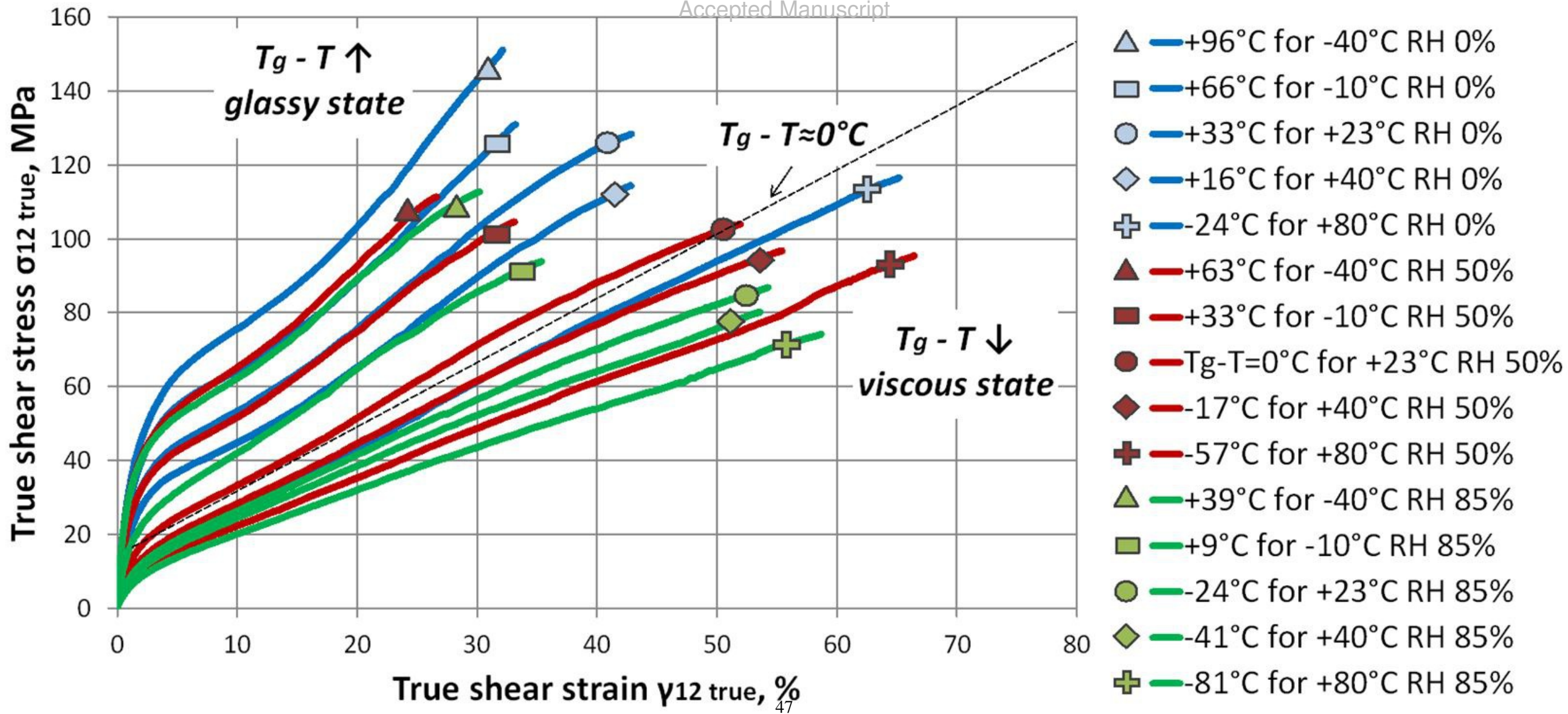
X

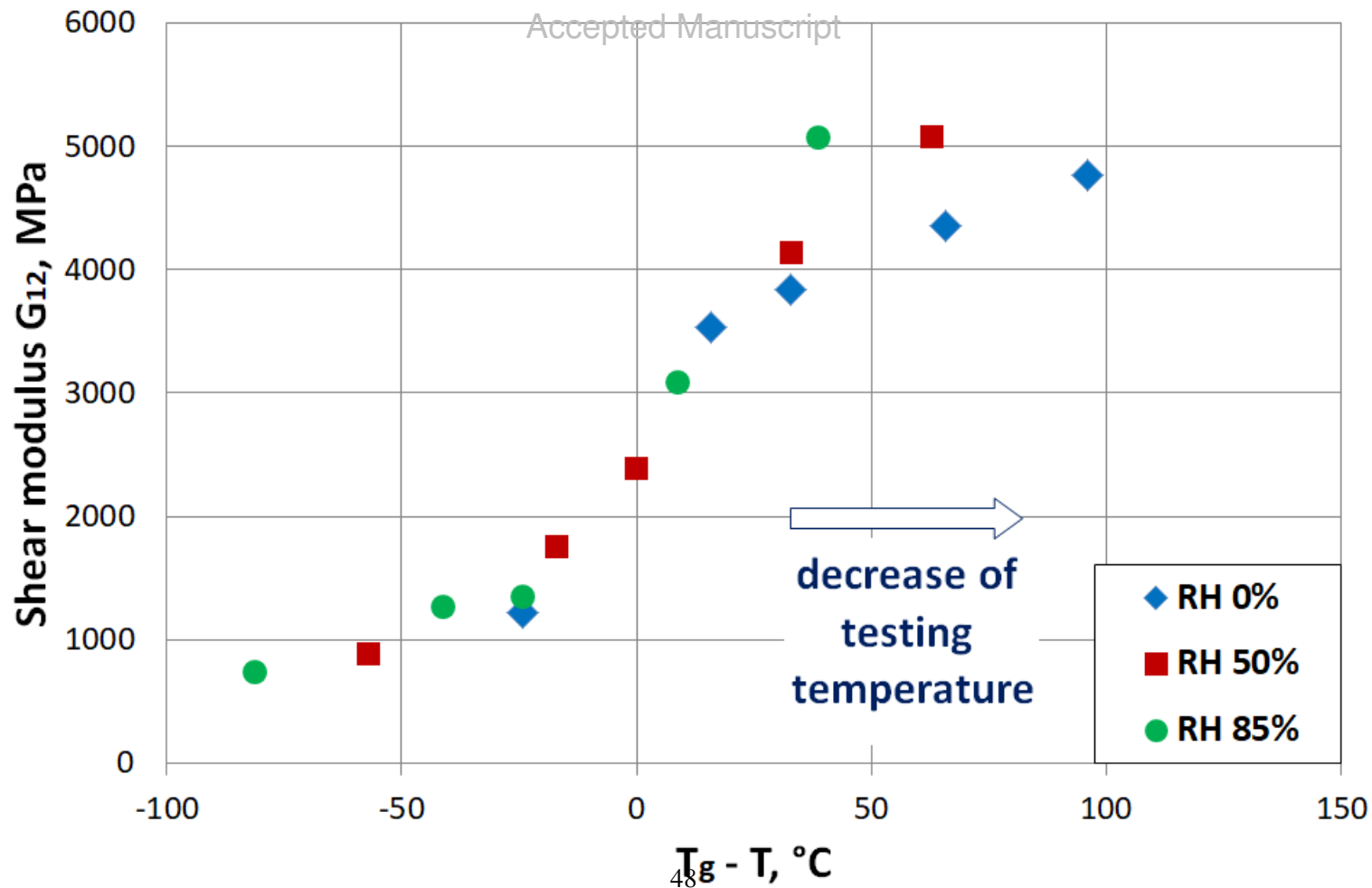
80c

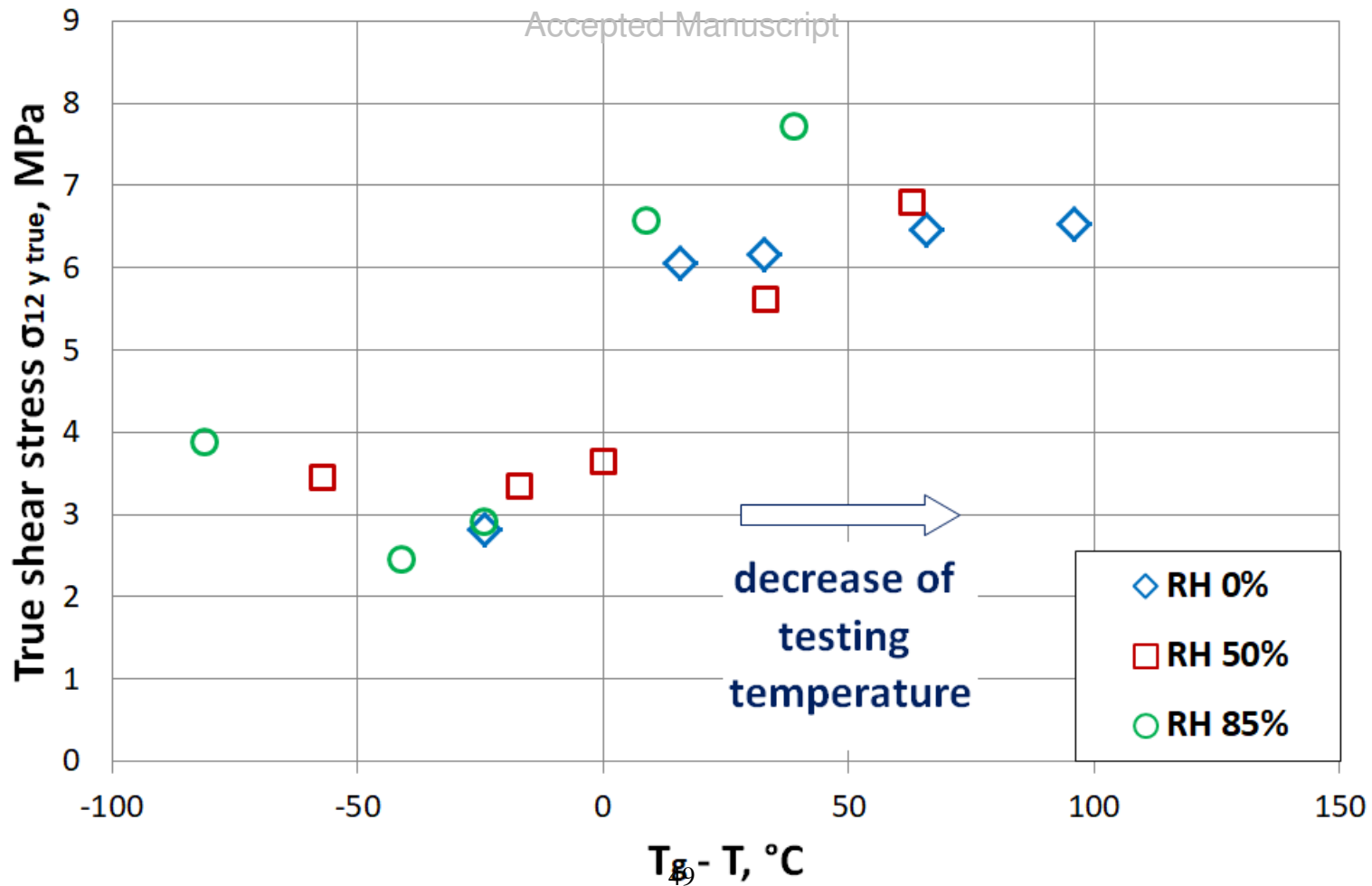












decrease of  
testing  
temperature

- ◇ RH 0%
- RH 50%
- RH 85%

5/HRO

-40°C

4/HRO

-40°C

3/HRO

-40°C

1/HRO

-40°C

6/HRS  
S

-40°C



12.15  
HR  
X  
80c

Loss in mass of reference specimens, %

